Received: 11 November 2018 | Revised: 13 December 2019 | Accepted: 16 December 2019

DOI: 10.1111/mec.15345

ORIGINAL ARTICLE

MOLECULAR ECOLOGY WILEY

Beyond the landscape: Resistance modelling infers physical and behavioural gene flow barriers to a mobile carnivore across a metropolitan area

Sophia E. Kimmig[1] | Joscha Beninde[2,3] | Miriam Brandt[1] | Anna Schleimer[4] | Stephanie Kramer-Schadt[1,5] | Heribert Hofer[1,6] | Konstantin Börner[1] | Christoph Schulze[7] | Ulrich Wittstatt[8] | Mike Heddergott[4] | Tanja Halczok[9] | Christoph Staubach[10] | Alain C. Frantz[4]

[1]Leibniz Institute for Zoo and Wildlife Research (IZW), Berlin, Germany

[2]Department of Biogeography, Trier University, Trier, Germany

[3]LA Kretz Center for California Conservation Science, Institute of the Environment and Sustainability, University of California, Los Angeles, CA, USA

[4]Musée National d'Histoire Naturelle, Luxembourg, Luxembourg

[5]Department of Ecology, Technische Universität Berlin, Berlin, Germany

[6]Freie Universität Berlin (FU), Berlin, Germany

[7]Landeslabor Berlin-Brandenburg (LLBB), Frankfurt (Oder), Germany

[8]Landeslabor Berlin-Brandenburg (LLBB), Berlin, Germany

[9]Universität Greifswald, Zoologisches Institut und Museum, Greifswald, Germany

[10]Friedrich-Loeffler-Institut, Federal Research Institute for Animal Health, Greifswald, Germany

Correspondence
Sophia Elisabeth Kimmig, Leibniz Institute for Zoo and Wildlife Research (IZW), Berlin, Germany.
Email: Sophia.Kimmig@gmail.com

Funding information
Stiftung Naturschutz Berlin, Grant/Award Number: J0067

Abstract

Urbanization affects key aspects of wildlife ecology. Dispersal in urban wildlife species may be impacted by geographical barriers but also by a species' inherent behavioural variability. There are no functional connectivity analyses using continuous individual-based sampling across an urban-rural continuum that would allow a thorough assessment of the relative importance of physical and behavioural dispersal barriers. We used 16 microsatellite loci to genotype 374 red foxes (*Vulpes vulpes*) from the city of Berlin and surrounding rural regions in Brandenburg in order to study genetic structure and dispersal behaviour of a mobile carnivore across the urban-rural landscape. We assessed functional connectivity by applying an individual-based landscape genetic optimization procedure. Three commonly used genetic distance measures yielded different model selection results, with only the results of an eigenvector-based multivariate analysis reasonably explaining genetic differentiation patterns. Genetic clustering methods and landscape resistance modelling supported the presence of an urban population with reduced dispersal across the city border. Artificial structures (railways, motorways) served as main dispersal corridors within the cityscape, yet urban foxes avoided densely built-up areas. We show that despite their ubiquitous presence in urban areas, their mobility and behavioural plasticity, foxes were affected in their dispersal by anthropogenic presence. Distinguishing between man-made structures and sites of human activity, rather than between natural and artificial structures, is thus essential for better understanding urban fox dispersal. This differentiation may also help to understand dispersal of other urban wildlife and to predict how behaviour can shape population genetic structure beyond physical barriers.

KEYWORDS

dispersal, functional connectivity, landscape of fear, landscape resistance modelling, RESISTANCEGA, urban ecology

1 | INTRODUCTION

Urbanization results in dramatic environmental change (Johnson & Munshi-South, 2017) and some species flourish in these semi-artificial ecosystems (Møller, 2009; Shochat, Warren, Faeth, McIntyre, & Hope, 2006). Yet, urbanization affects key aspects of wildlife ecology such as survival, foraging and reproductive success (Wilson et al., 2016). Moreover, it has a substantial impact on the movement ecology and dispersal ability of populations (Johnson & Munshi-South, 2017; Tucker et al., 2018). Urban species may for example be restricted by geographical barriers and become reproductively isolated (Gortat, Rutkowski, Gryczynska, Kozakiewicz, & Kozakiewicz, 2017; Lourenço, Álvarez, Wang, & Velo-Antón, 2017). The physical structure of the urban environment is thus likely to have an impact on dispersal capacity (Bohonak, 1999).

However, the urban environment imposes much more on wildlife than the need to navigate a highly altered landscape. Animals often perceive humans as predators and avoid areas of human activity (Samia, Nakagawa, Nomura, Rangel, & Blumstein, 2015). Individuals from the rural surroundings of an urban area might thus face a behavioural barrier to enter urbanized areas. Within the city, species with the physical capability of crossing the urban matrix may face behavioural barriers if they avoid man-made objects (with their artificial structures or scents) or human presence per se. Different scenarios are thus conceivable for population structure and drivers of gene flow across the urban-rural continuum and the perception of human-induced risks may differentiate urban and rural populations beyond physical barriers. The role of behavioural limitations to movement has been frequently overlooked. Examining the functional connectivity—the connectivity of the landscape from the species' perspective (Tischendorf & Fahrig, 2000)—of the urban landscape would thus help to assess the relative importance of physical and behavioural dispersal barriers and thereby make an important contribution to understanding the ecology and evolution of wildlife in novel environments.

Molecular genetic methods permit inferences about wildlife dispersal without the need to collect extensive field data on individual movements (Frantz, Do Linh San, Pope, & Burke, 2010; Guillot, Leblois, Coulon, & Frantz, 2009). Recently, numerous studies of gene flow in urban areas have been published, but many of those focus on smaller and less mobile species that are thought to face major barriers in urban areas (Beninde, Feldmeier, Veith, & Hochkirch, 2018; Combs, Puckett, Richardson, Mims, & Munshi-South, 2018; Munshi-South, 2012). Studies on larger and more vagile species, in contrast, analysed the population genetic structure of animals from peripheral suburban populations or from isolated sampling sites within urban and rural areas (Blanchong, Sorin, & Scribner, 2013; Santonastaso, Dubach, Hauver, Graser, & Gehrt, 2012; Stillfried, Fickel, et al., 2017; Wandeler, Funk, Largiadèr, Gloor, & Breitenmoser, 2003). There is currently no thorough analysis of the population and landscape genetic structure of a vagile species in an urban-rural continuum available, using continuous individual-based sampling. This would permit to identify drivers of urban gene flow, including those unrelated to the physical properties of the landscape.

Landscape genetic methods are particularly suited to assess functional connectivity. Specifically, hypotheses on how the environment influences gene flow in a target species can be evaluated by statistically relating the distribution of genetic similarities among individuals to landscape characteristics (Cushman, McKelvey, Hayden, & Schwartz, 2006; Schwartz et al., 2009). Several statistical problems have been recently solved, such as the nonindependence among ecological distances and the subjective assignment of resistance values to environmental features (Peterman, 2018; Prunier, Colyn, Legendre, Nimon, & Flamand, 2015; Sawyer, Epps, & Brashares, 2011). Landscape genetic approaches are still evolving (Balkenhol, Waits, & Dezzani, 2009; Manel & Holderegger, 2013; Richardson, Brady, Wang, & Spear, 2016) and some methodological aspects remain relatively underexplored. For example, while a simulation study by Shirk, Landguth, and Cushman (2017) has suggested that not all genetic distance measures perform equally well in model selection, different genetic distance measures have not been tested with the same empirical data set.

Aiming to gain a more fundamental understanding of the impact of urbanization on wildlife populations at a large spatial scale, we here focus on a mobile mesopredator, the red fox (*Vulpes vulpes*). Red foxes are ecologically flexible (Voigt & Macdonald, 1984) and occur in various habitat types. Their populations prosper even in highly urbanized habitats. In Berlin, our focal city, the first reports of foxes date from the 1950s (Saar, 1957) and by the 1990s the entire city was populated (Börner, Wittstatt, Schneider, 2009). Their ubiquitous distribution in highly artificial and fragmented areas as well as their movement ecology make foxes an ideal model for this study. On the one hand, foxes are very mobile. Urban animals have been reported to routinely cross streets and even rivers (Adkins & Stott, 1998) and gene flow may be unhampered by the urban landscape. On the other hand, anthropogenic infrastructure could represent significant gene flow barriers for mobile carnivores (Riley et al., 2006) and both telemetry and genetic studies point towards the existence of distinct urban and rural fox populations (Janko et al., 2011; Wandeler et al., 2003).

Here, we used continuous sampling of individuals both within Berlin as well as the adjoining rural countryside to evaluate three hypotheses. (a) The null hypothesis was that, due to their niche breadth and mobility, foxes disperse unhampered throughout the city and urban and adjoining rural populations are panmictic. This predicts that the urban fabric has no influence on gene flow, resulting in the absence of population and landscape genetic structure. (b) The fragmentation hypothesis posits that fox dispersal was (solely) affected by physical barriers such as rivers, built-up areas and highways. Under this hypothesis, multiple physical barriers limit gene flow, resulting in several scattered genetic populations. (c) The urban island hypothesis (Gloor, Bontadina, Hegglin, Deplazes & Breitenmoser, 2001) expects that dispersal may (also) be affected by behavioural barriers, which are most likely to occur at the border of the city where the rural landscape changes into the urban environment. Accordingly,

individuals within the city are habituated to manmade structures and human presence, while individuals from the rural surroundings are not and thus face a behavioural barrier to enter the urban area. This predicts two genetic populations resulting from limited gene flow across the city border. We further expect that urban foxes disperse along artificial structures and through built-up areas when crossing the urban matrix.

In order to examine these predictions, we used assignment-based population genetic approaches to identify the location of abrupt genetic discontinuities and resistance-modelling-based landscape genetic approaches to assess the functional connectivity of the landscape. We tested three genetic distance measures to address the performance of different genetic distance measures in model selection and to generate robust results.

2 | MATERIALS AND METHODS

2.1 | Study area, sampling and laboratory procedures

The Berlin metropolitan area (Figure 1a) has 3.5 million inhabitants and covers ~900 km^2. It has been steadily changing during the last century and independent villages and satellite agglomerations were incorporated into the city. Thus, the urban landscape structure is quite heterogeneous, ranging from extremely urbanized areas of dense housing and high proportions of impervious surfaces to districts where forests and lakes represent up to 75% of land cover. The city area includes around 2,500 city parks, some areas of agricultural cultivation, 160 km^2 of forest and several lakes. The countryside around Berlin is characterised by sparse urban agglomerations, agriculture and forest. The landscape transition from the countryside to (sub-)urban areas does not fully correspond to the administrative boundaries between Berlin and Brandenburg as there are several forests, lakes and green areas that reach into the city (Figure 1b). These green spaces and lakes are commonly used as recreational areas.

Between 2010 and 2015, tissue samples from 374 foxes were collected (Figure 1a): Within Berlin, 188 fox carcasses were collected for a municipal disease monitoring program. For each individual, location (street, house number/km, postal code), sex and age category were known. The 186 samples from rural Brandenburg were collected by hunters and made available to the veterinary authorities or the authors of this study. No animal was killed with the aim of providing samples for this study. For 116 Brandenburg samples, the location or the cadastral unit of origin was known, for the remaining 70 individuals, only the nearest village to the harvest site was recorded. In these cases, we chose a random forest location within 2 km of the village recorded as sampling site. No information on sex and age was available for the samples from Brandenburg.

Tissue samples were stored at −20°C or in absolute ethanol. We genotyped the samples using 16 microsatellite loci: DGN3, DGN14, FH2541, REN161A12, REN162B09, REN69B24, V374, V402, V502, Vv-C01.424, Vv-C08.618, Vv-CPH11, Vv-CPH2, Vv-INU055, VVM124, VVM189 (Breen et al., 2001; Mariat, Amigues, & Boscher, 1998; Moore, Brown, & Sacks, 2010; Wandeler & Funk, 2006; Yan et al., 2015). The data are publicly available (see Data Accessibility). Detailed information on laboratory procedures is given in Appendix S1.

2.2 | Population genetic analysis

To assess the suitability of the microsatellites for population genetic analyses, we tested each locus for deviations from Hardy-Weinberg and linkage equilibrium using GENEPOP v.4.7.0 (Rousset, 2008). We also used GENEPOP to calculate F_{IS} values (Weir & Cockerham, 1984). To avoid deviations resulting from Wahlund effects and isolation-by-distance (Frantz, Cellina, Krier, Schley, & Burke, 2009), when analysing the full data set, we subsampled the complete data set to generate 10 data sets consisting of 24 spatially clustered individuals (details in Appendix S2). We tested each set for significant deficiency or excess of heterozygotes and linkage disequilibrium (LD) among loci using the Markov chain method in GENEPOP with 10,000 dememorization steps, 20 batches and 5,000 subsequent iterations. We used the false discovery rate (FDR) to account for multiple tests (Verhoeven, Simonsen, & McIntyre, 2005).

We used two Bayesian-based clustering methods to estimate the number of genetic subpopulations (K), STRUCTURE v. 2.3.4 (Pritchard, Stephens, & Donnelly, 2000) and GENELAND v. 3.3.2 (Guillot, Estoup, Mortier, & Cosson, 2005). Running conditions and specifications are described in Appendix S3. We used Microsatellite analyser MSA 4.05 (Dieringer & Schlötterer, 2003) to calculate observed and expected heterozygosities and the number of alleles across all loci. The level of genetic differentiation between genetic clusters inferred by STRUCTURE and GENELAND was assessed using F_{ST} (Weir & Cockerham, 1984) in SPAGEDI 1.4 (Hardy & Vekemans, 2002); significance was tested with 10,000 permutations of individual genotypes between populations. We analysed the complete data set using the Estimated Effective Migration Surfaces (EEMS) method (Petkova, Novembre, & Stephens, 2016). It uses georeferenced genetic data and can identify locations of abrupt genetic discontinuities (i.e., gene flow barriers) in data sets characterised by isolation-by-distance patterns (details in Appendix S4). We plotted the results for the run with the highest log-likelihood, using the REEMSPLOTS package in R (Petkova et al., 2016).

2.3 | Landscape resistance modelling

Functional connectivity was assessed using RESISTANCEGA 3.1-3 (Peterman, 2018). It calculates pairwise resistance distances between individuals and uses a linear mixed effects model based on genetic algorithms to maximize the fit of resistance surfaces to the

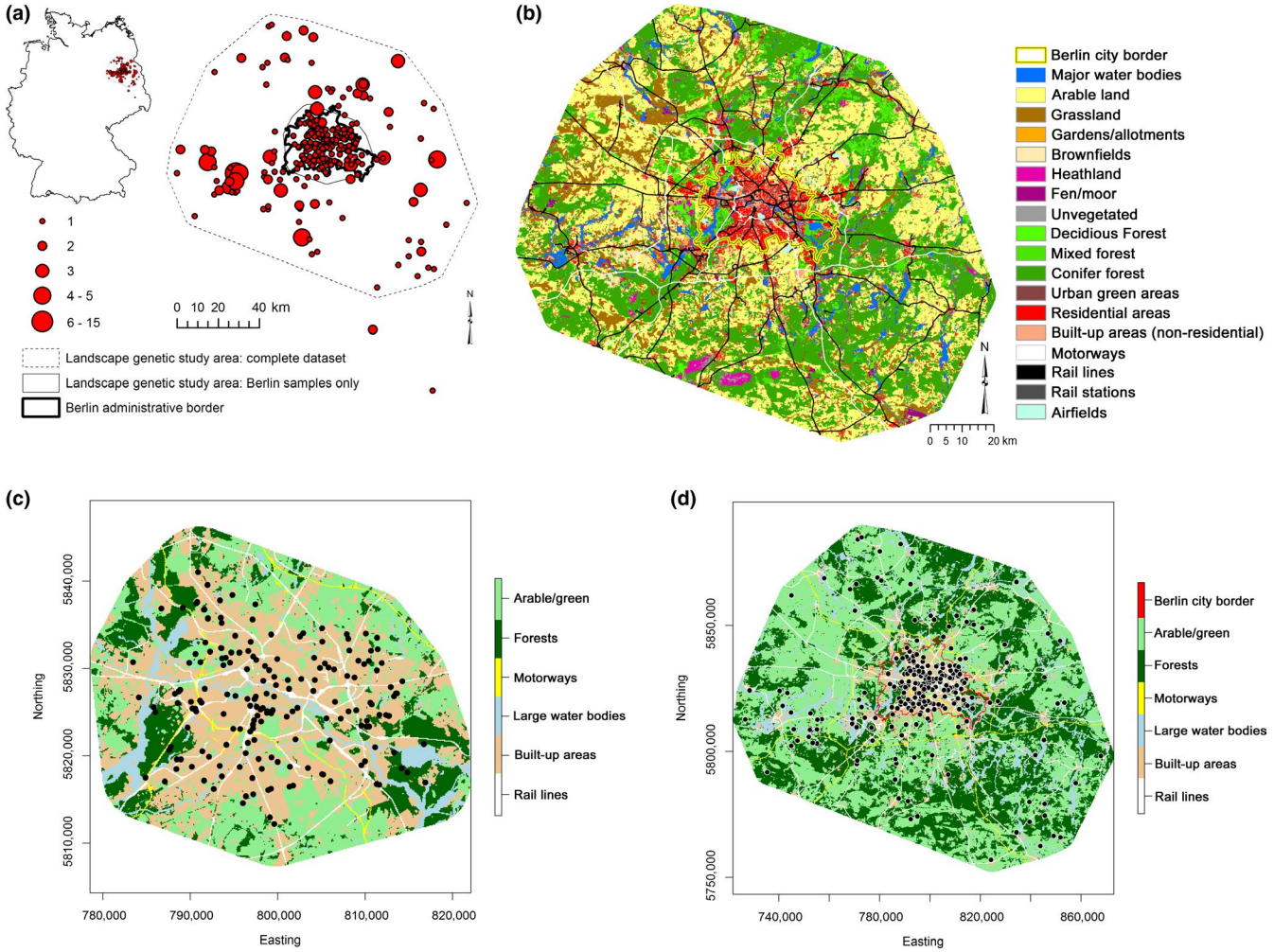

FIGURE 1 Sample distribution and land cover maps of the study area. (a) The location of the study area within Germany and the geographic origin of samples, with size of the circles indicative of the number of samples collected from a locality. The dotted- and thin-lined polygons show the boundaries of the study area used in landscape resistance modelling for the complete data set and the Berlin-only data set, respectively. (b) Land cover map of the landscape genetics study area. (c) Habitat categories considered in the genetic landscape resistance modelling of the city of Berlin, with the black dots showing the location of the 184 samples that were included in the analysis. (d) Habitat categories considered in the genetic landscape resistance modelling of Berlin and the surrounding countryside, with the black dots showing the location of the 286 samples that were included in the analysis. Habitat data were taken from the German authoritative topographic cartographic information system (ATKIS) [Colour figure can be viewed at wileyonlinelibrary.com]

data. The process is based on stochastic search algorithms that solve optimisation problems by mimicking processes of natural selection (Scrucca, 2013). The optimisation process uses log-likelihood as the objective function. Mixed models were fitted using the maximum likelihood population effects (MPLE) parameterization (Clarke, Rothery, & Raybould, 2002) implemented in the R package lme4 (Bates, Mächler, Bolker, & Walker, 2014). A simulation study by Shirk, Landguth, and Cushman, (2018) has shown that this linear-mixed-effects-model-based method had a high accuracy in model selection.

RESISTANCEGA can optimise categorical and continuous resistance surfaces, as well as multiple resistance surfaces simultaneously (Peterman, 2018). All analyses in this work were based on categorical resistance surfaces and the commute-time geographic resistance distance (Kivimäki, Shimbo, & Saerens, 2014), equivalent to circuit-theory-based resistance distances (McRae, Shah, & Mohapatra, 2013). Model fit was assessed with the corrected Akaike information criterion (AIC_c): A specific model was considered a better fit if the difference in AIC_c (ΔAIC_c) to the next model was >2 AIC_c units. To check for convergence, each optimisation run in the study was performed twice for each landscape feature or combination of landscape features. Using the GA.PREP() function, we set the maximum value to be assessed during optimization of categorical resistance surfaces to 500 and retained all other default parameters of the GA.PREP() function.

We performed separate analyses for foxes sampled within Berlin and the full data set including the surrounding countryside. We split the analysis because subtle behavioural patterns within the urban area may be missed in a joint analysis of the complete data set. Also, the greater precision of sampling locations within Berlin allowed a fine-scale analysis of the permeability of the urban environment (see

below). Except when mentioned, ARCMAP v.10.3 (ESRI Inc) was used to prepare resistance surfaces. Potential movements of individuals at the edge of the study area can be artificially constrained by the proximity to the boundary (Koen, Garroway, Wilson, & Bowman, 2010). The extent of the study areas was therefore obtained by plotting a minimum convex polygon around the sampling locations. Then, based on dispersal distances obtained by capture-mark-recapture methods (Harris & Trewhella, 1988; Trewhella & Harris, 1990) we added a 5 km buffer around this feature.

Landscape classification was based on the German topographic cartographic information system ATKIS (Figure 1b, Gruenreich, 1992). Seven landscape categories, hereafter called environmental predictors, were considered to potentially influence gene flow (Figure 1c–d, Figure S1). (a) *arable/green*: all types of arable land and grassland, fallow land, allotments, airports, public parks, cemeteries and bare soils; (b) *built-up areas*: residential, industrial and commercial areas; (c) the *city border* of Berlin (or variations thereof; see below); (d) *forests*: irrespective of their composition; (e) *motorways*: with tunnelled sections within the city not considered; (f) *railways*: including major stations but excluding tramways and (g) larger *water bodies*: including lakes and major rivers (which do not overlap with other shapes), excluding small streams, creeks and underground canals (line elements that overlap other shapes). For the initial analyses within the city area only, we pooled all arable land, green and forests into a single (h) *all vegetation* layer (Figure 1c; Figure S2). To distinguish the actual landscape from environmental predictors used for functional connectivity analysis, environmental predictors appear in italics throughout the text.

In addition to ATKIS, we used data from the 2012 Copernicus Urban Atlas (https://land.copernicus.eu/) that uses high-resolution remote sensing data to provide detailed land cover information of larger European urban areas and their hinterland. It comprised 27 different land cover types (Table S1), of which six, classified under *urban fabric*, give an indication of the degree of imperviousness of land cover (Montero, Van Wolvelaer, & Garzón, 2014). We used the following (nonoverlapping) categories of the Urban Atlas to subdivide the *built-up area* layer within the city (see Figure S3): (a) *Continuous urban fabric* (sealing level (S.L.) >80%), (b) *discontinuous dense urban fabric* (S.L. 50%–80%), (c) *discontinuous medium dense urban fabric* (S.L. 30%–50%), (d) *industrial, commercial, public, military and private units* and (e) a pooled layer consisting of *discontinuous low density urban fabric* (S.L. 10%–30%), *discontinuous very low density urban fabric* (S.L. <10%) and all the remaining built-up areas not covered by the previous categories.

We converted all layers into grids. Not considering cells without data, each cell in the initial grid had a value of zero or one, depending on whether it contained a feature under consideration. For linear predictors and *water bodies* we used a priority rule, meaning that every grid cell containing a linear predictor was coded as belonging to that predictor, independently of the proportion of the cell it covered. For shape predictors, we used a majority rule, with the cell being attributed to the single predictor with the largest area within the cell. Grid cell size was set to 250 × 250 m, giving rise to 233,798 grid cells without 'no data' cells, when ignoring three geographic outliers (Figure 1a). Since we only considered one animal per grid cell, this resulted in 286 individuals being included in the analysis. Given the ecology of the species and the occasional lack of precision of the location information, we considered this to be an adequate compromise between computation time and spatial resolution. When focusing on the individuals in Berlin only, grid cell size was set to 100 × 100 m, given the higher accuracy of the sampling location and the smaller size of the study area. This resulted in 125,728 grid cells without "no data" cells, and 184 individuals being analysed.

2.4 | Genetic distance measures

Interindividual genetic distance measures are not equally accurate in model selection, especially when faced with weaker genetic structure (see Shirk et al., 2017). We therefore compared the performance of three measures: (a) genetic distances based on Factorial Correspondence Analysis (FCA), an eigenvector-based multivariate analysis closely related to principal component analysis (PCA); (b) Nei's genetic distance applied to individuals (D_{Nei}, Nei & Takezaki, 1983), as used by Beninde et al. (2016) and (c) the proportion of shared alleles between two individuals averaged over loci (D_{PS}, Bowcock et al., 1994), that is frequently used in landscape resistance modelling (Landguth et al., 2010; Trumbo, Spear, Baumsteiger, & Storfer, 2013). FCA clusters variance between loci into composite gradients. It accentuates differences between individuals better than measures that weight all loci equally. The latter includes D_{PS}, which uses the number of direct differences between genotypes. D_{Nei} considers allele frequencies when calculating genetic distances and ranges from 0 for identical genotypes to 1 when genotypes are completely dissimilar.

We used GENETIX v. 4.05.2 (Belkhir, 2004) to perform an FCA on a multiple contingency table of the genetic data and used the first 10 FCA axes as a compromise between model accuracy and noise generation (Shirk et al., 2017). We calculated an Euclidean distance matrix for all individuals from their values on each FCA axis using the R package Ecodist (Goslee & Urban, 2007) and refer to this distance measure as "FCA". We used the R packages Alleles in Space (Miller, 2005) to calculate D_{Nei} and Adegenet (Jombart, 2008) to calculate D_{PS}.

2.5 | Optimisation of resistance surfaces: Single categorical environmental predictors

We first used the SS_OPTIM() command in RESISTANCEGA to optimise the resistance of single categorical environmental predictors and test model selection performance of the genetic distance measures. In order to complete these analyses within a reasonable time, we limited initial tests to the seven ATKIS predictors (five for Berlin only). We performed a (pseudo-)bootstrap procedure using the RESIST.BOOT() command, which subsamples individuals and resistance matrices without replacement at each iteration, refits the MLPE model to different

resistance distance matrices and recalculates AIC_c scores. We sampled 75% of the observations at each iteration. This was done in order to assess the relative support of each optimised resistance surface and the robustness of the model selection results given different sample combinations. For each genetic distance measure, we assessed model fit based on the differences between corrected Akaike information criterion (ΔAIC_c) values. When comparing genetic distance measures, the measure that gave rise to the highest marginal R^2 values (while generating biologically meaningful results) was considered the most adequate.

2.6 | Multiple resistance surfaces

After optimising individual categorical resistance surfaces, the relevant variables must be combined into a composite resistance surface. This is necessary to test whether models with several landscape features are better supported than models with single landscape features and, ultimately, to gain an understanding of the functional connectivity of the entire landscape (Khimoun et al., 2017; Ruiz-Lopez et al., 2016).

2.7 | Multiple resistance surfaces: Automatically combining categorical predictors

We used the samples from Berlin, the best genetic distance measure and the five ATKIS categories to compare two approaches that combine categorical predictors into a single surface. Firstly, we used RESISTANCEGA's ALL _ COMB() wrapper function which automatically combines and optimises all possible combinations of the five categorical predictors and runs the RESIST.BOOT() command to conduct a bootstrap analysis. However, the MS _OPTIM() command gives different resistance values to a linear feature depending on which other feature it overlaps with, which may lead to erroneous conclusions (Section 3).

2.8 | Multiple resistance surfaces: Single-surface optimisation for combining categorical predictors

We therefore also tested a second approach for combining categorical predictors into a single surface: Rather than letting RESISTANCEGA automatically combine different surfaces, we applied the single-surface optimisation (SS _OPTIM()) procedure to resistance grids containing multiple environmental predictors, i.e. each grid contained *N* categorical predictors and each cell in the grid had a value ranging from zero to *N*, depending on whether it was classified as one of the *N* predictors or whether it was classified as *matrix*, i.e., the remaining uniform study area not containing the features under investigation. We will refer to these grids as "multicategorical" surfaces (to differentiate them from composite surfaces obtained using ALL _ COMB()). The principle underlying the multicategorical models is to add individual predictors based on model support (AIC_c values) but to only retain a new predictor if its addition improved support ($\Delta AIC_c > 2$ after a RESIST.BOOT() bootstrap analysis). Individual predictors whose model support was $\Delta AIC_c < 2$ with *distance* were not considered. The optimisation for each feature or combination of features was performed twice and only included the distance matrix from the optimisation run with the lowest AIC_c value in bootstrap analysis. We will refer to this as the "stepwise optimisation" procedure.

2.9 | Multiple resistance surfaces: Dealing with overlapping linear features

In order to assess the effect of the overlap of linear predictors, we considered all possible priority combinations of predictors. We tested, for example, individual surfaces where linear predictor 1 took precedence over linear predictor 2 at points of overlap and vice versa. We also tested the support of a surface where all points of overlap between linear features were classified as a distinct feature. In each case, the combination with the highest model support after bootstrapping was retained for further analysis.

2.10 | Multiple resistance surfaces: Effect of initial cell values of multicategorical surfaces

Preliminary exploratory analyses suggested that in the stepwise optimisation, the initial cell values of a predictor influenced the optimised resistance value for the predictors (and hence model support). We therefore coded individual predictors relative to their resistance/permeability inferred in the initial individual analysis. For example, in order to obtain the highest model support when manually combining two different categorical predictors in a single grid, a predictor inferred to be permeable had to be given a grid value of zero, a predictor resisting gene flow a grid value of two and all other cells a value of one. In order to test more formally whether the optimised resistance values were sensitive to the starting values of the input surface, we took multicategorical surfaces with different combinations of predictors that were retained in the stepwise optimisation procedure and inverted the values of the input surface. We performed a total of four independent optimisation runs for each initial and inverted surface.

2.11 | Multiple resistance surfaces: Optimising multicategorical surfaces of Berlin

After these initial tests based on ATKIS categories *all vegetation*, *built-up areas*, *water bodies*, *motorways*, *railways*, we refined the composite Berlin model further. We performed single-surface optimisation for both the *forest* and *arable/green* layers (which had been previously pooled in *all vegetation*) as well as the five Urban Atlas categories of *built-up areas* to test model support of each individual layer. We then followed a stepwise optimisation procedure to generate a multicategorical surface. If the difference in model support between individual predictors was $\Delta AIC_c < 2$, we

added both predictors individually and jointly to the previous multicategorical model and only retained the model with the highest support.

2.12 | Multiple resistance surfaces: Optimising multicategorical surfaces of the whole study area

We also used a stepwise procedure to generate a multicategorical surface for the whole Berlin/Brandenburg study area. To gain a more detailed assessment of the interface between the city and the surrounding countryside as a possible gene flow barrier, we created a concave hull of the administrative city border using the ConcaveHull plug-in for QGIS (QGIS Development Team, 2018). We then drew 1, 2, 3, 4 and 5 km buffers around the concave hull and used the SS _ OPTIM() command in RESISTANCEGA to separately optimise the resistance of all five inner and outer borders (Figure S4). We then used the boundary model with the highest support together with the six remaining ATKIS predictors to identify the best-supported multicategorical surface. Again, we performed the RESIST. BOOT() bootstrap analysis for each optimisation run, to circumvent potential problems with imprecise locations of individuals sampled in Brandenburg.

The best-supported multicategorical resistance surfaces for the Berlin and Berlin/Brandenburg data sets were used to predict movement/gene flow patterns across both study areas using CIRCUITSCAPE v.4.0.5 (McRae, 2006). Animal movement paths were inferred between all pairs of sample location as well as between 200 random locations generated for both data sets using ARCMAP v.10.3 and located along the border of the study areas.

3 | RESULTS

After correction for multiple tests, locus V502 deviated from Hardy-Weinberg equilibrium (HWE) in five out of 10 subsampled data sets (Table S2), its F_{IS} values ranging between 0.40–0.53 in these five data sets. The locus was thus excluded from further analyses. No other locus showed systematic deviation from HWE. Some loci were in linkage disequilibrium in some subsampled data sets, but no pair deviated more than once (Table S3). We therefore performed further population genetic analyses with all loci except V502.

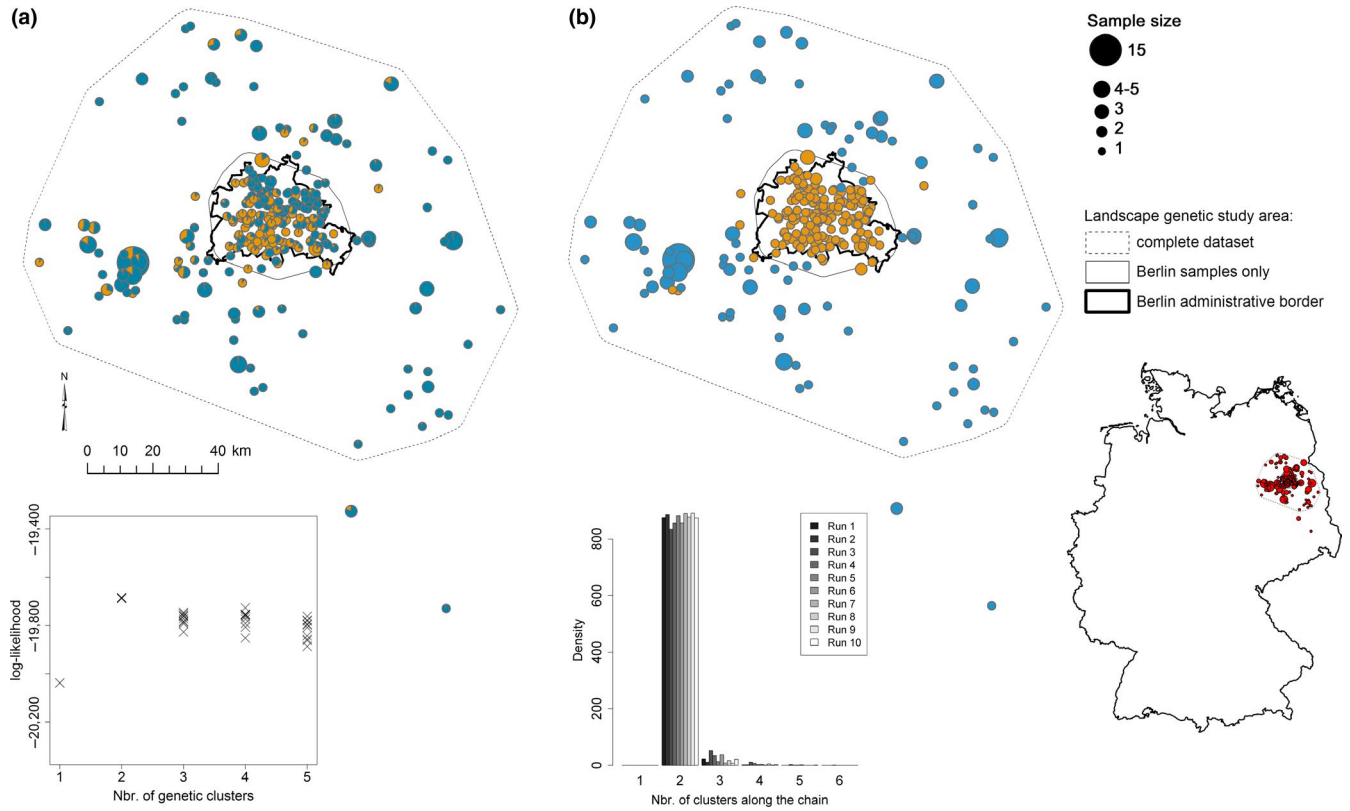

FIGURE 2 Geographic distribution of the population genetic clusters. (a) STRUCTURE results: plot of the number of clusters against their estimated log-likelihood (bottom) and geographic representation of the $K = 2$ assignment analysis (top). The pattern of the pie chart indicates the assignment probabilities averaged across all individuals sampled in the same location, with the two different colours representing membership of different clusters and the size indicating the number of collected samples from one locality. (b) GENELAND results: plot of the number of clusters inferred by the ten initial GENELAND runs (bottom) and geographic representation of the modal assignment to one of the two clusters, i.e., the pattern of the pie chart indicates the proportion of individuals from a locality assigned to one of the two clusters (top). Bottom right insert shows the location of the study area within Germany [Colour figure can be viewed at wileyonlinelibrary.com]

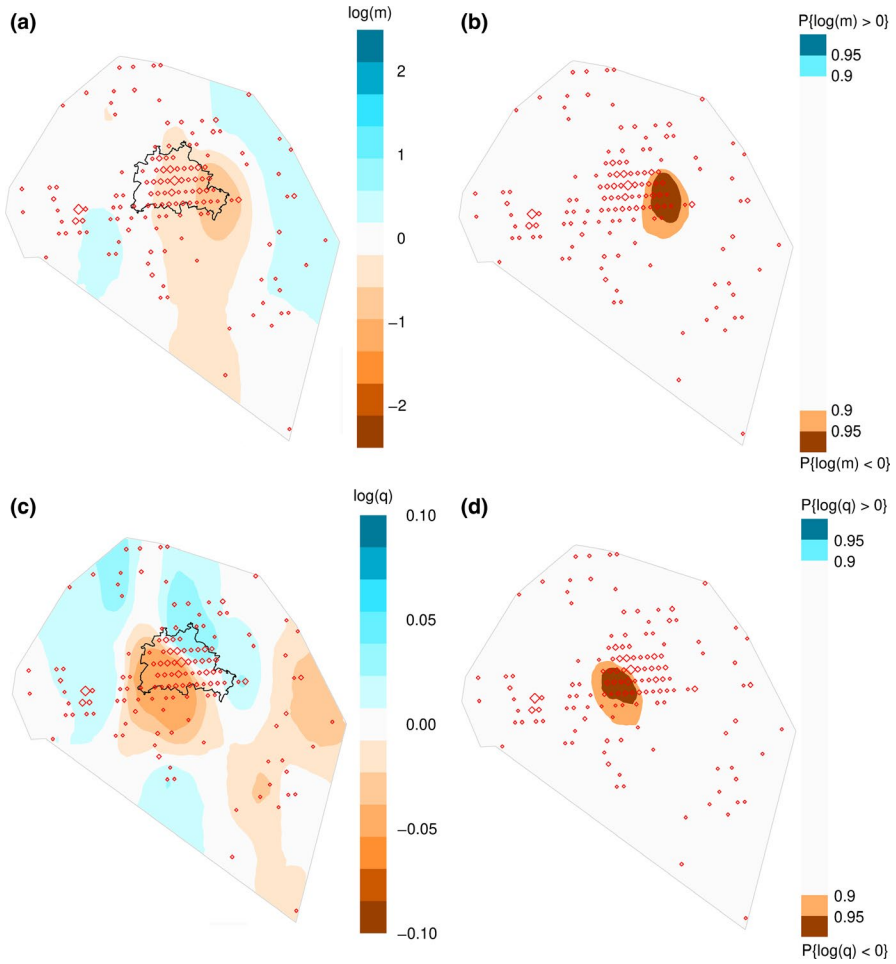

FIGURE 3 EEMS-estimated effective migration and diversity rates. (a) Interpolated surface of the posterior mean migration rates m (on a $\log_{10}$ scale) depicting deviations from continuous gene flow. Negative values in red indicate areas of reduced migration rates, whereas positive values in blue indicate higher-than-expected migration rates. (b) Plot highlighting regions where the effective migration rates are significantly higher (highlighted in blue) or lower (highlighted in orange) than the overall average rate. (c) Interpolated surface of the posterior mean diversity rates q (on a $\log_{10}$ scale) depicting effective diversity across the study area. Diversity rates q describe the genetic dissimilarity between distinct individuals from the same deme. Negative values in red indicate areas of diversity, whereas positive values in blue indicate higher-than-expected diversity. (d) Plot highlighting regions where the effective diversity rates are significantly higher (highlighted in blue) or lower (highlighted in orange) than the overall average rate. A total of 1,000 demes were used in the analyses [Colour figure can be viewed at wileyonlinelibrary.com]

3.1 | Population structure

The log-likelihood values inferred by STRUCTURE provided clear support for the presence of two genetic clusters (Figure 2a). The corresponding clusters approximately consisted of (a) samples collected in the centre, west and south of Berlin and (b) samples from all rural localities and north-eastern Berlin, yet their precise geographic distribution was not clear-cut (Figure 2a; Figure S5). The location of the genetic discontinuity identified by STRUCTURE approximately corresponds to the course of the rivers Spree and Havel (Figure S5). GENELAND also inferred $K = 2$ as the most likely number of clusters in each of the 10 initial runs (Figure 2b). The samples assigned to one cluster almost all originated from within the Berlin city border, whereas the second cluster contained samples almost exclusively collected in the countryside (Figure 2b), i.e., GENELAND identified an urban and a rural cluster, with the boundary quite accurately corresponding to the administrative city border. The EEMS contour plot of effective migration rates identified a band of (slightly) reduced long-distance migration rates that covered most of the city, but also extended to the south of the study area (Figure 3a). In the east of Berlin, migration rates were significantly lower than the overall average rate (Figure 3b).

Independently of the clustering method, the more urban cluster had reduced genetic diversity compared to the rural cluster (Table S4) and the clusters were significantly differentiated from each other. Differentiation between both STRUCTURE clusters ($F_{ST} = 0.026$; $p < .0001$) was higher than between the two GENELAND clusters ($F_{ST} = 0.011$; $p < .0001$). The EEMS contour plot of effective diversity illustrated that in southwest Berlin effective diversity rates were significantly lower than the overall average rate (Figure 3c, d).

3.2 | Optimisation of resistance surfaces: Single categorical environmental predictors

When considering the five ATKIS environmental predictors, the results obtained after bootstrapping (Table 1) were qualitatively similar to initial model results (Table S5). The three genetic distance measures did not converge on the same results in the model selection process (Table 1). In the analyses using D_{Nei} and D_{PS}, *motorways* was always identified as the most significant factor facilitating gene flow, with *railways* ranked as second best model (also facilitating gene flow) and all other models (except one: *water bodies* in one run using the D_{PS} genetic measure) having a difference in $\Delta AIC_c < 2$ with the *distance* model. In the FCA, the difference between the *distance* model and all five predictors was large ($\Delta AIC_c > 6.2$), with the ranking of the five models remaining identical between the two independent optimisation runs (Table 1). The *water bodies* model that best explained gene flow with

the FCA measure (*water bodies* being a strong gene flow barrier) had an average marginal R^2 of 0.289, a substantially higher model fit than the best model's average marginal R^2 of 0.057 and 0.054 for D_{Nei} and D_{PS}, respectively. We therefore used FCA for further analyses.

3.3 | Multiple resistance surfaces: Automatically combining categorical predictors

When considering the prebootstrapping results of the optimisation of all possible combinations of the five single ATKIS environmental predictors (ALL_COMB() function, Table S6), only three combinations had a $\Delta AIC_c > 2$ below the best single-feature model (*water bodies*). After bootstrapping, 11 combinations had a $\Delta AIC_c > 2$ below the *water bodies*-only model, with the best model containing *railways* and *water bodies* (resistance values: *railways*: 1, *matrix*: 185, overlap *water bodies/railways*: 250, *water bodies*: 434; Table S7; Figure S6). When simultaneously optimising and overlaying different categorical resistance surfaces that included linear features, RESISTANCEGA gave different resistance values to a linear feature depending on which feature it overlapped with. For example, in the model that included all five environmental predictors, RESISTANCEGA optimised the resistance value of 24 different categorical features (Figure S7).

3.4 | Multiple resistance surfaces: Single-surface optimisation for combining categorical predictors & dealing with overlapping linear features

The two best-supported models in the FCA-based analysis of individual features were *water bodies* and *railways*. When combining these two predictors in a single-surface optimisation, the highest model support was obtained (after bootstrapping) when giving *water bodies* precedence over *railways* in the resistance grid (when *water bodies* overlap with *railways*, the cell is classified as water body; Table S8). When adding the next best-supported *motorways* model to the single-surface analysis, the highest model support was obtained when *water bodies* took precedence over *motorways* and *motorways* took precedence over *railways* (*water bodies* > *motorways* > railways; Table S9). After bootstrapping, the three best "overlap" models had almost identical model support ($\Delta AIC_c < 2$; Table S9). *Water bodies* always strongly impeded gene flow, while *railways* and *motorways* conducted gene flow. When adding *all vegetation* (and hence *built-up areas*) to each of these three overlap models in a single-surface analysis, the model with *water bodies* > *motorways* > railways was again the best-supported model after bootstrapping (Table S10). In summary, when only considering the ATKIS data, the best permeability model for Berlin included all five tested features (Table 2; Figure S8). *Water bodies* strongly resisted gene flow (resistance: 1574), *railways* (resistance: 1) and *motorways* (resistance: 4) enhanced gene flow. *Built-up areas* (resistance: 291) were more permeable than *all vegetation* (resistance: 494). The following analyses were based on the *water bodies* > *motorways* > railways overlap model.

3.5 | Multiple resistance surfaces: Effect of initial cell values of multicategorical surfaces

Multicategorical models whose starting cell values had been inverted gave rise to different optimised resistance values for the predictors and had a lower model support than the noninverted original multicategorical surfaces (Table S11).

3.6 | Multiple resistance surfaces: Optimising multicategorical surfaces of Berlin

When repeating single-feature optimisations but splitting the *all vegetation* predictor into the two predictors *forest* and *arable/green* and the *built-up areas* into the five Urban Atlas categories, *water bodies*, *railways* and *motorways* were still the individual features with the highest model support (Table 2), with *arable/green* generating a better model support than the *all vegetation* model (Table 2). Similarly, two Urban Atlas land cover categories (*sealing levels* [*S.L.*] of 30%–50% and >80%) had higher model support than the predictor including all built-up areas (Table 2). The fourth-best (*arable/green*) and the fifth-best (*S.L.* 50%–80%) individual models had similar model support ($\Delta AIC_c = 0.5$; Table 2). The resistance value inferred for each single predictor is given in Table S12. A better-supported model was obtained when adding *S.L.* 30%–50% to the *water bodies*, *railways*, *motorways* ("*mrw*") model than when adding the *arable/green* predictor or both *arable/green* and *S.L.* 30%–50% to the *mrw* model (Table 2). Adding further single-feature predictors to the single-feature optimisation procedure in order of decreasing support (and testing all possible combinations when $\Delta AIC_c < 2$ between two individual predictors) resulted in three multicategorical models having comparable support (Table 2). The overall best model (Figure 4) included *railways* (inferred resistance value: 1), *motorways* (resistance: 2), *S.L.* 30%–50% (resistance 8), *S.L.* 50%–80% (resistance: 103), *S.L.*>80% (resistance: 469), water bodies (resistance: 784) as well as the remaining *matrix* (resistance: 282). Despite differences in the resistance surface values between the models, the CIRCUITSCAPE current maps for the best supported model and the model with the fewest predictors were very similar, both suggesting that gene flow within the city of Berlin mostly occurred along linear landscape elements (*railways* and *motorways*, Figure 4).

3.7 | Multiple resistance surfaces: Optimising multicategorical surfaces of the whole study area

All *city border* models and obtained better support than the distance only model and inferred the city border to resist gene flow (Table

TABLE 1 Boostrap results of the single-predictor RESISTANCEGA analysis for the city of Berlin

	Run 1					Run 2				
Predictor	**avg. AIC_c**	***k***	**ΔAIC_c**	**avg.weight**	**avg.mR^2**	**avg. AIC_c**	***k***	**ΔAIC_c**	**avg.weight**	**avg.mR^2**
(a) Nei's genetic distance (D_{Nei})										
Motorways	−21,765.0	3	0	0.977	0.035	−21,770.8	3	0	0.977	0.036
Railways	−21,750.0	3	15.0	0.016	0.057	−21,755.5	3	15.3	0.016	0.057
Built-up areas	−21,747.9	3	17.1	0.002	0.017	−21,753.4	3	17.4	0.002	0.017
Water bodies	−21,747.9	3	17.1	0.002	0.022	−21,753.3	2	17.5	0.002	0.018
Distance	−21,747.8	2	17.2	0.002	0.018	−21,753.3	3	17.5	0.002	0.022
All vegetation	−21,747.7	3	17.3	0.001	0.018	−21,753.2	3	17.6	0.001	0.018
(b) Proportion of shared alleles (D_{PS})										
Motorways	−21,744.2	3	0	0.418	0.025	−21,761.1	3	0	0.946	0.034
Railways	−21,741.1	3	3.1	0.228	0.054	−21,748.9	3	12.2	0.038	0.054
Water bodies	−21,740.6	3	3.6	0.258	0.051	−21,746.5	3	14.6	0.004	0.017
Built-up areas	−21,738.7	3	5.5	0.036	0.017	−21,746.3	2	14.8	0.004	0.018
Distance	−21,738.5	2	5.7	0.031	0.018	−21,746.2	3	14.9	0.004	0.017
All vegetation	−21,738.4	3	5.8	0.029	0.017	−21,746.1	3	15.0	0.004	0.020
(c) Ten-axes-based factorial correspondence analysis (FCA)										
Water bodies	130,757.2	3	0	0.701	0.289	130,743.3	3	0	0.707	0.289
Railways	130,771.3	3	14.1	0.222	0.057	130,759.2	3	15.9	0.206	0.057
Motorways	130,779.9	3	22.7	0.076	0.014	130,766.9	3	23.6	0.087	0.014
All vegetation	130,800.7	3	43.5	0.001	0.030	130,787.4	3	44.1	<0.001	0.027
Built-up areas	130,803.4	3	46.5	<0.001	0.029	130,790.3	3	47.0	<0.001	0.029
Distance	130,810.0	2	52.8	<0.001	0.007	130,796.9	2	53.6	<0.001	0.007

Notes: Three different genetic distance measures (a–c) and five environmental predictors from the German authoritative topographic cartographic information system (ATKIS) were compared (Section 2). The initial model results are presented in Table S5. To check for convergence, each optimisation was performed twice for each landscape feature (Run 1 & Run 2). Avg. AIC_c, average of the AICc values obtained for each model in 1,000 bootstrap iterations; ***k***, number of parameters; **ΔAIC_c**, difference in the avg. AIC_c values between the best supported model (lowest avg. AIC_c) and each subsequent model; Avg.weight, average of the AIC_c weights obtained for each model in 1,000 bootstrap iterations; Avg.mR^2, average marginal R^2 of 1,000 bootstrap iterations. Predictors are sorted according to increasing avg.AIC_c values

S13). The best-supported model (the city border converted into a concave hull) had a marginal R^2 of 0.42. The *city border concave* was also the most significant single predictor influencing gene flow when considering all other predictors (Table 3; Figure S9). Considering the bootstrapping results of the FCA-based genetic distance only, five of the six remaining single-feature models better explained gene flow than the distance only model (the exception being *motorways*; Table 3). Forest and arable/green were the only environmental features inferred to facilitate gene flow (Table S14). Again, the three genetic distance measures did not converge on the same results in the model selection process (Table 3), with the support of the *city border* model in particular changing with the genetic distance measure considered. Also, the marginal R^2 values obtained with D_{Nei} and and D_{PS} were considerably lower than those obtained with the FCA-based measure (Table 3).

When performing a stepwise procedure to create a multicategorical surface, two multicategorical models had almost identical support. The overall best-supported model (after bootstrapping) contained *city border concave*, *built-up areas*, *railways* and *water bodies* (Table 4), where *water bodies* took precedence over *railways* (Table S15). While *railways* (resistance: 1) and the remaining habitat *matrix* (resistance: 2) enhanced gene flow, *city border concave* (resistance: 498) and *water bodies* (resistance: 70) provided a greater resistance than *built-up areas* (resistance: 6). The second-best model (with almost identical support) had the same predictors (with similar resistance values) but did not include *railways*. Considering both models, the CIRCUITSCAPE maps did not show a clearly-defined corridor network in the Brandenburg countryside (Figure S9).

4 | DISCUSSION

In the present work, we aimed to assess the importance of physical and behavioural dispersal barriers to drive population and landscape genetic structure of the red fox across the Berlin metropolitan area. We found support for the fragmentation hypothesis with major water bodies and densely built-up areas resisting gene flow. Contrary to our prediction, however, these barriers did not create several scattered populations across the city, possibly

TABLE 2 Results of the multicategorical functional connectivity analysis for the city of Berlin

Predictors	avg.AIC_c	*k*	ΔAIC_c	avg.weight	avg.mR^2
Water*Railways*Motorways*S.L.30%–50%*S.L.50%–80%*S.L. > 80%	130,726.1	8	0	0.194	0.169
Water*Railways*Motorways*S.L.30%–50%*S.L.50%–80%*S.L. > 80%*Industry	130,726.7	9	0.6	0.244	0.199
Water bodies*Railways*Motorways* S.L.30%–50%*S.L. > 80%	130,727.4	7	1.3	0.153	0.188
Water bodies*Railways*Motorways*S.L.30%–50%	130,730.2	6	4.1	0.044	0.168
Water*Railways*Motorways*S.L.30%–50%*S.L. > 80% *Industry	130,730.6	8	4.5	0.115	0.184
Water*Railways*Motorways*S.L.30%–50%*S.L.50%–80%*S.L. > 80% *Remaining built-up	130,731.8	9	5.7	0.072	0.152
Water*Railways*Motorways*S.L.30%–50%*S.L. > 80% *Remaining built-up	130,731.9	8	5.8	0.030	0.150
Water*Railways*Motorways*All vegetation*Built-up areas	130,736.5	6	10.4	0.031	0.157
Water bodies*Railways *Motorways*Arable/green	130,738.2	6	12.1	0.039	0.113
Water bodies*Railways*Motorways*Arable/green*S.L.30%–50%	130,738.3	7	12.2	0.058	0.220
Water bodies*Railways *Motorways	130,741.7	5	15.6	0.011	0.195
Water bodies*Railways	130,749.5	4	23.3	0.005	0.087
Water bodies	130,769.1	3	43.0	0	0.293
Railways	130,784.0	3	57.9	0	0.057
Motorways	130,792.9	3	66.8	0.003	0.014
Arable/Green	130,800.5	3	74.3	0.001	0.049
S.L.30%–50%	130,801.6	3	75.4	0	0.017
S.L. > 80%	130,809.1	3	83.0	0	0.051
All vegetation	130,813.7	3	87.6	0	0.030
S.L.50%–80%	130,815.5	3	89.4	0	0.038
Built up areas	130,816.5	3	90.4	0	0.029
Industry	130,817.4	3	91.3	0	0.030
Remaining built-up	130,820.8	3	94.7	0	0.023
Forest	130,822.9	3	96.8	0	0.009
Distance	130,823.1	2	97.0	0	0.007

Notes: The best-supported multicategorical surfaces combining different environmental predictors were obtained using a stepwise procedure: Individual predictors were added based on model support (corrected Akaike information criterion values, AIC_c), but only retained if their addition improved support of the multicategorical model ($\Delta AIC_c > 2$). Presented here are the bootstrapping results based on two optimisation runs (Table S12) that were performed for each (combination of) landscape features. avg. AIC_c, average of the AIC_c values obtained for each model in 1,000 bootstrap iterations; *k*, number of parameters; ΔAIC_c, difference in the avg; AIC_c, values between the best supported model (lowest avg.AIC_c) and each subsequent model; avg.weight, average of the AIC_c weights obtained for each model in 1,000 bootstrap iterations; avg.mR^2, average marginal R^2 of 1,000 bootstrap iterations. Predictors are sorted according to increasing avg.AIC_c values. S.L., sealing level

because motorways and railways served as movement corridors. We also found support for the urban island hypothesis and inferred limited gene flow across the city border, indicating an effect of behavioural barriers. Urban foxes further made use of artificial structures when dispersing through the urban matrix. Our results may thus suggest a hierarchy of drivers of genetic structure with a general behavioural effect and impediment through physical barriers underneath. However, the specifics of our results also suggest that genetic structure was relatively weak and, therefore, dispersal rates still high.

4.1 | Population genetic structure and gene flow

The genetic clustering algorithms both inferred $K = 2$ as the mostly likely number of subpopulations, yet they differed in the spatial distribution of the clusters. For GENELAND, the cluster boundary closely coincided with the administrative city border, whereas for STRUCTURE the urban cluster mostly excluded the north and north-east of the city. The location of the STRUCTURE-inferred genetic discontinuity approximately corresponded to the course of the rivers Spree and Havel (Figure S5). EEMS also identified reduced

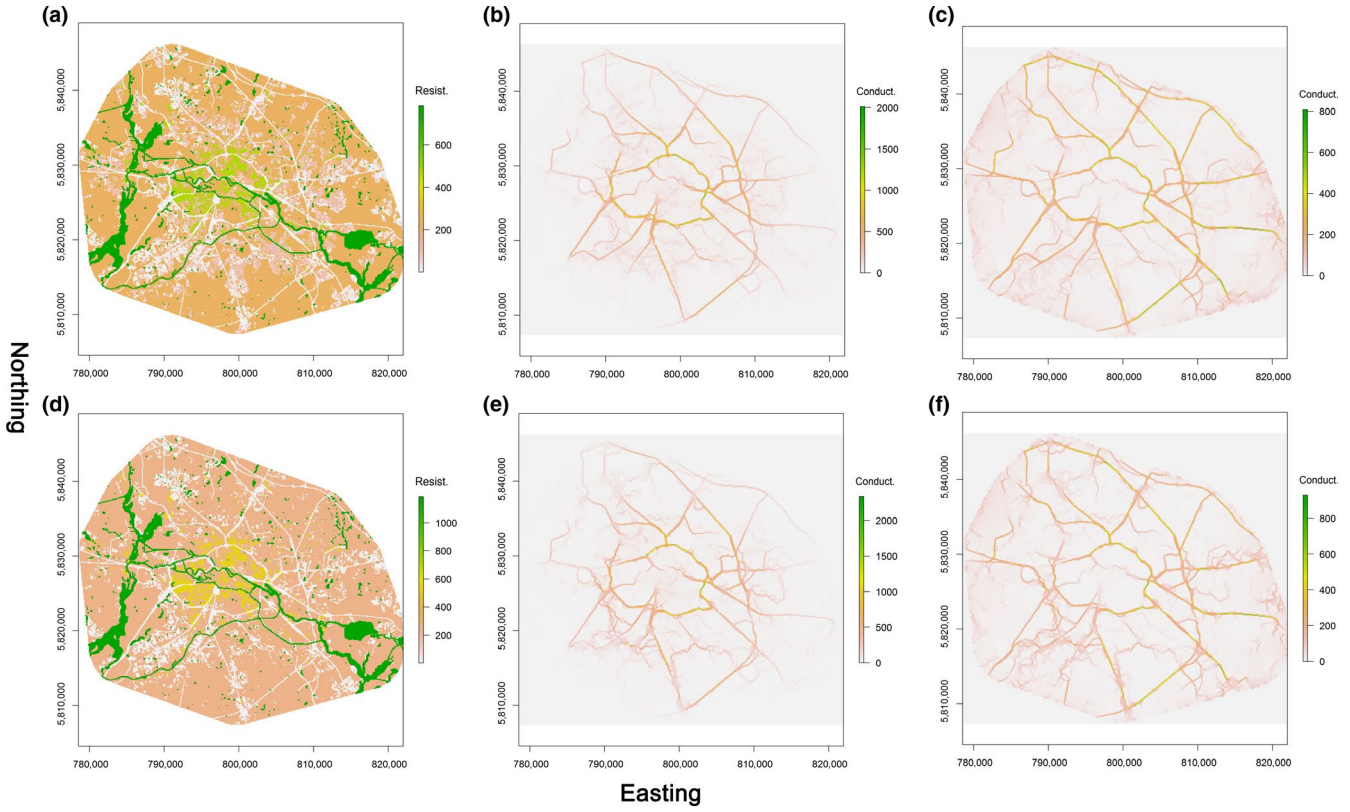

FIGURE 4 Cartographic representation of results from genetics-based resistance modelling for foxes in the city of Berlin. (a) Optimised resistance surface of the overall best multicategorical model and the corresponding Circuitscape connectivity map showing conductance to gene flow based on (b) the sample locations and (c) sampling locations simulated at the edge of the study area. (d) Optimised resistance surface of the best-supported multicategorical model with fewest predictors and the corresponding Circuitscape connectivity map showing conductance to gene flow based on (e) the sample locations and (f) sampling locations simulated at the edge of the study area [Colour figure can be viewed at wileyonlinelibrary.com]

migration (broadly) around the city of Berlin, but especially in East Berlin. Despite discrepancies, all three population genetic methods inferred the presence of a cluster located within the confines of the city. Furthermore, the landscape resistance modelling identified (a concave hull of) the administrative city border as the main barrier to fox dispersal in the study area (Figure S9). Finally, the F_{ST}-based approach and the EEMS method confirmed reduced genetic diversity within (parts of) the city compared to the surrounding countryside. Our results therefore provided general support for a genetic differentiation between urban and rural areas, i.e., the urban island hypothesis.

While the three population genetic methods inferred the presence of an urban island, they differed in its proposed location and composition. Different solutions for the partitioning of a data set may result from differences in the assumptions and algorithms underlying the statistical methods (Guillot et al., 2009) and the way they deal with weak or hierarchical genetic structure (Frantz et al., 2006; Puechmaille, 2016; Rowe & Beebee, 2007) as well as with deviations from random mating that are not due to physical barriers (e.g., isolation-by-distance, presence of relatives, Rodríguez-Ramilo & Wang, 2012). As all three methods inferred a 'circular' cluster in the centre of the sampling distribution and the diversity within the city was reduced, it appears unlikely that the partitioning was an artefact of an isolation-by-distance pattern (Frantz et al. 2009). Perhaps the most likely explanation for the observed outcome is that population genetic structure is weak because of high dispersal rates in our vagile study species. A simulation study suggested that STRUCTURE was efficient at inferring the correct number of genetic clusters even at lower levels of genetic differentiation (i.e., F_{ST} = 0.02–0.03), but this was not necessarily the case for its accuracy in assigning individuals to these clusters (Latch, Dharmarajan, Glaubitz, & Rhodes, 2006). While, by definition, GENELAND infers abrupt genetic discontinuities, the deviation from IBD inferred by EEMS also appeared to be relatively slight (Figure 3). We therefore conclude that our results provided evidence for genetic differentiation between urban and rural foxes, but that dispersal between urban and rural areas was ongoing.

4.2 | Performance of genetic distance measures

While RESISTANCEGA offers high potential to gain a species-specific understanding of the functional connectivity of the landscape, careful consideration of some technical aspects seems necessary. In the present study, the fit of a model testing single categorical environmental predictors and its rank relative to other predictors clearly differed between genetic distance measures. In the simulation study by Shirk et al. (2017) most metrics performed equally

TABLE 3 Boostrap results of the single-predictor RESISTANCEGA analysis for the complete data set

	Run 1					Run 2				
Predictor	avg. AIC_c	*k*	ΔAIC_c	avg.weight	avg.mR^2	avg. AIC_c	*k*	ΔAIC_c	avg.weight	avg.mR^2
(a) Nei's genetic distance (D_{Nei})										
Built-up areas	310,883.2	3	0	0.838	0.008	310,901.4	3	0	0.824	0.008
Forests	310,890.0	3	6.8	0.156	0.014	310,907.9	3	6.5	0.171	0.014
Arable/green	310,904.2	3	21.0	0.003	0.009	310,922.6	3	21.2	0.004	0.009
City border concave	310,929.6	3	46.4	0.003	0.016	310,947.6	3	46.2	0.002	0.017
Water bodies	310,938.6	3	55.4	<0.001	0.014	310,957.3	3	55.9	<0.001	0.014
Railways	310,942.3	3	59.1	<0.001	0.010	310,960.7	3	59.3	<0.001	0.010
Motorways	310,955.9	3	72.7	<0.001	0.028	310,974.2	3	72.8	<0.001	0.028
Distance	310,956.8	2	73.6	<0.001	0.012	310,975.3	2	73.9	<0.001	0.011
(b) Proportion of shared alleles (D_{PS})										
Built-up areas	310,892.3	3	0	0.956	0.007	310,921.3	3	0	0.951	0.007
Forests	310,902.5	3	10.2	0.039	0.011	310,931.4	3	10.1	0.044	0.011
Arable/green	310,909.8	3	17.5	0.004	0.008	310,939.1	3	17.8	0.004	0.008
City border concave	310,937.3	3	45.0	0.001	0.014	310,967.0	3	45.7	<0.001	0.014
Railways	310,943.9	3	51.6	<0.001	0.010	310,973.3	3	52.0	<0.001	0.010
Water bodies	310,944.2	3	51.9	<0.001	0.013	310,973.7	3	52.4	<0.001	0.013
Distance	310,956.4	2	64.1	<0.001	0.012	310,985.5	3	64.2	<0.001	0.026
Motorways	310,956.7	3	64.4	<0.001	0.026	310,985.9	2	64.6	<0.001	0.012
(c) Ten-axes-based factorial correspondence analysis (FCA)										
City border concave	310,842.9		0	0.663	0.389	310,860.3	3	0	0.721	0.386
Built-up areas	310,878.6		35.7	0.211	0.058	310,899.7	3	39.4	0.170	0.057
Forests	310,889.3		46.4	0.095	0.054	310,910.6	3	50.3	0.089	0.052
Arable/green	310,910.9		68.0	<0.001	0.038	310,931.4	3	71.1	0.001	0.037
Water bodies	310,921.5		78.6	0.031	0.172	310,941.0	3	80.7	0.020	0.170
Railways	310,954.5		111.6	<0.001	0.065	310,973.9	3	113.6	<0.001	0.064
Motorways	310,990.1		147.2	<0.001	0.027	311,010.0	3	149.7	<0.001	0.011
Distance	310,991.0		148.1	<0.001	0.012	311,010.1	2	149.8	<0.001	0.011

Notes: Three different genetic distance measures and seven environmental predictors from the German authoritative topographic cartographic information system (ATKIS) were compared (Section 2). The initial model results are presented in Table S14. To check for convergence, each analysis was performed twice for each landscape feature (Run 1 & Run 2). avg. AIC_c, average of the AIC_c values obtained for each model in 1,000 bootstrap iterations; *k*, number of parameters; ΔAIC_c, difference in the avg; AIC_c values between the best supported model (lowest AIC_c) and each subsequent model; avg.weight, average of the AIC_c weights from 1,000 bootstrap iterations; avg.mR^2, average marginal R^2 of 1,000 bootstrap iterations. Predictors are sorted according to increasing avg.AIC_c values

well in model selection accuracy, except in situations of low genetic structure and small sample size. The discrepancies between genetic distance measures reported here are therefore consistent with high dispersal rates.

Shirk et al. (2017) performed Principal Components Analyses (PCA) on multiple contingency tables and found that genetic distances based on multiple-axes PCA maximise model selection accuracy, with other measures performing almost as well in cases of high levels of genetic structure. PCA assumes continuous, normally distributed data (Dytham, 2011), whereas Factorial Correspondence Analysis (FCA) was designed for multistate categorical variables (She, Autemm, Kotulas, Pasteur, & Bonhomme, 1987) and is thus more suitable for the analysis of allele states. Analogous to Shirk et al. (2017), our 10-axes FCA metric led to a better model fit (in terms of marginal R^2) than the other two measures and generated biologically meaningful results. Future research will show whether this is a general feature of FCA and how much this depends on the number of axes included. With a modest strength of the genetic signal, a few large eigenvectors may have insufficient diagnostic power to infer more subtle processes. The geographical distribution of the target species may also matter (Shirk et al., 2017). We considered 10 axes to be a good compromise between accuracy and noise and (almost)

TABLE 4 Results of the multicategorical functional connectivity analysis for the complete data set

Predictors	avg.AIC_c	*k*	ΔAIC_c	avg.weight	avg.mR^2
City border concave*Built-up areas*Water bodies*Railways	310,624.2	6	0	0.475	0.373
City border concave*Built-up areas*Water bodies	310,624.4	5	0.2	0.371	0.384
City border concave*Built-up areas	310,665.4	4	41.2	0.008	0.397
City border concave*Built-up areas*Arable/Green	310,668.6.	5	44.3	0.138	0.481
City border concave*Built-up areas*Forest	310,675.7	5	51.5	0.008	0.340
City border concave	310,810.5	3	186.3	<0.001	0.384
Built-up areas	310,851.2	3	226.9	<0.001	0.057
Forest	310,862.3	3	238.0	<0.001	0.053
Arable/Green	310,883.1	3	258.9	<0.001	0.037
Water bodies	310,893.7	3	269.5	<0.001	0.170
Railways	310,925.5	3	301.3	<0.001	0.065
Motorways	310,961.1	3	336.9	<0.001	0.027
Distance	310,961.7	2	337.5	<0.001	0.012

Notes: The best-supported multicategorical surfaces combining different environmental predictors were obtained using a stepwise procedure: Individual predictors were added based on model support (corrected Akaike information criterion, AIC_c, values), but only retained if their addition improved support of the multicategorical model ($\Delta AIC_c > 2$). Presented here are the bootstrapping results based on two optimisation runs (summarised in Table S15) that were performed for each (combination of) landscape features. avg. AIC_c, average of the AICc values obtained for each model in 1,000 bootstrap iterations; *k*, number of parameters; ΔAIC_c, difference in the avg; AIC_c, values between the best supported model (lowest avg.AIC_c) and each subsequent model; avg.weight, average of the AIC_c weights obtained for each model in 1,000 bootstrap iterations; avg.mR^2, average marginal R^2 of 1,000 bootstrap iterations. Predictors are sorted according to inceasing avg.AIC_c values

all single ATKIS predictors had better model support than the distance model alone.

4.3 | Pitfalls in landscape resistance modelling

Our results show that a subtle understanding of gene flow requires the simultaneous consideration of multiple landscape features. However, an issue that emerged as nontrivial was the generation of composite resistance surfaces that include linear features. When considering multiple linear features, model support may depend on the rule for classifying a grid cell where linear features overlap. The comparison of all combinations of environmental predictors using the ALL _ COMB() command was hampered by the way the input grids were created. As we applied a priority rule to linear and a majority rule for shape predictors, they frequently overlapped when generating composite surfaces. This led to the creation of separate categories for each type of overlap and decreased model support. Without a priority rule the linear features would have been interrupted in the input grid. A different option could be to create single-feature input grids by reclassifying a grid containing all features. This poses the problem of how to deal with overlapping linear features and linear features that run in parallel.

As a solution to these dilemmas, we adopted the multicategorical approach where we applied the single-surface optimisation procedure to grid surfaces containing multiple environmental predictors. This allowed us to explicitly test different overlap scenarios. In combination with the stepwise approach of creating multicategorical surfaces, this required fewer optimisation runs than the comparison of all possible combinations using ALL _ COMB(). This might be an important consideration when having a large(r) number of predictors. A drawback of the multicategorical approach was that model support and optimised resistance values were sensitive to starting values of the input surface. The method(s) for simultaneously considering multiple landscapes therefore need(s) to be chosen carefully.

Finally, the layers in this study were very general. For example, we assumed that every stretch of motorway as well as every Urban Atlas category had a consistent effect on gene flow over space and time. We are well aware that this approach reflects the actual structure of the habitat only to some extent, especially in the urban area: The already highly heterogeneous structure of a rapid growing metropolis like Berlin is subject to permanent fluctuation. These processes cannot be reflected in the spatial data set and sometimes the same environmental predictors may even have opposite effects on gene flow. A highway in Berlin, for example, may be a strong barrier

if it is fenced-in and rarely interrupted by bridges or underpasses. In contrast, the same motorway may serve as a corridor on other stretches, if it is combined with long, continuous green strips connecting highly fragmented built-up areas. Consequently, those layers can only serve as an approximation of the functional connectivity of the real landscape. Nevertheless, this may still yield valuable insights into dispersal processes.

4.4 | The urban island

Our results provided general support for a genetic differentiation between urban and rural areas, i.e. the urban island hypothesis. The observed genetic structure was relatively weak, indicating that some individuals from the surrounding areas do disperse into Berlin. With abundant high-quality food and a lack of hunting pressure, the city is possibly a better-quality habitat for foxes, despite an increased mortality. Urban foxes could therefore be expected to stay within the city and individuals from the surrounding areas to disperse into the urban area. However, there was no support for a constant influx of foxes from the countryside and the (genetic) exchange between the urban agglomeration and the rural countryside was sufficiently reduced to maintain genetic structure. In line with this, a radio-tracking study of foxes in Zurich showed limited movement across an the urban-rural boundary (Gloor, 2002). Colonising urban areas may thus require behavioural shifts such as an improved tolerance of the presence of humans (Gloor et al., 2001). Such behavioural changes have often been interpreted as resulting from phenotypic plasticity, allowing habituation to humans (Bateman & Fleming, 2012; Kauhala, Talvitie, & Vuorisalo, 2016; Vuorisalo, Talvitie, Kauhala, Bläuer, & Lahtinen, 2014). However, work on urban birds suggested that avoidance of humans may have a genetic basis and urban colonisation may result from selection for fearless individuals (Carrete et al., 2016; Carrete & Tella, 2009; Møller et al., 2015). The presence of a genetically distinct urban population may thus result from a founder effect followed by limited urban-rural exchange due to differences in avoidance behaviour (see also below).

Given the political history of Berlin, there remains another explanation for the presence of an urban cluster: Between 1961 and 1989 the "Berlin Wall" (partially following the river Spree) separated West Berlin from eastern Berlin and the surrounding federal state of Brandenburg. While a founder effect may have created an initial reduction in genetic diversity among urban foxes, impermeable border fortifications could have limited gene flow and thus artificially maintained genetic differentiation between urban and rural foxes. However, genetic exchange between urban and rural foxes must also have remained sufficiently low in the ensuing 30 years to maintain genetic structure (with generation time being 2–3 years, DeCandia et al., 2019). Based on F_{ST} values ($F_{ST} \geq 0.027$), Wandeler et al. (2003) detected genetic differentiation between urban and rural foxes for the then recently (15 years) established fox population within Zurich. However, assignment tests provided evidence for ongoing urban-rural gene flow. A recent re-analysis of the same data set identified only one evolutionary cluster (DeCandia et al., 2019). Further research in other metropolitan areas might help to clarify whether the urban island is a general phenomenon or a specificity of Berlin.

4.5 | Gene flow within the cityscape

Gene flow in Berlin foxes was hampered by physical barriers. The landscape resistance models identified major water bodies as the most significant predictor resisting gene flow in the urban area. Contrary to our predictions, foxes did not freely move through the urban landscape. The best-supported multicategorical model(s) inferred highly urbanised areas (sealing levels >80%) to represent an important impediment to gene flow. On the other hand, urban fox dispersal did not depend on corridors of natural vegetation as it was described for other species (Goldingay et al., 2013; Munshi-South, 2012) either. While suburban areas with low degrees of imperviousness were inferred to be more permeable for dispersers than densely built-up areas, our results suggest that railways and motorways served as the main dispersal corridors. This last result is in line with results from radio-tracking studies in Edinburgh where railway lines were the main conduit for long-distance dispersal of male foxes (Kolb 1984).

Railway lines and motorways are highly artificial structures. On the circular railway around the city centre, trains pass continuously day and night. Similarly, the multilane motorways connecting the districts of Berlin are extremely busy with high-speed traffic. While railway-tracks are usually embedded within vegetated verges, motorways are not, and generally, dispersal along such transport infrastructure carries a high mortality risk (200–250 road-killed foxes are found in Berlin each year: Börner, 2014). Yet, what both landscape elements have in common (besides their linearity), is the absence of human activity, in terms of pedestrians and cyclists. The green spaces of Berlin, in contrast, are usually crowded. Although the actual mortality risk in green spaces and sparse built-up areas is low, they show less conductance to gene flow than motorways and railways (Figure 3), despite the latter's inherent mortality risk. Consequently, foxes may use artificial structures as corridors but avoid areas of human activity (see also Table 5). Adkins and Stott (1998) reported that city foxes stayed shy and preferably used sites when human activity was low. The authors concluded that foxes do not avoid human constructions—but humans themselves. Beyond physical barriers, human activity may thus represent a significant impediment to dispersal in urban foxes.

4.6 | The landscape of fear

Over centuries, foxes have been intensively hunted by humans - and still are. Although no hunting is conducted within the city, foxes should thus maintain a certain level of "background fear" (see

TABLE 5 Detected landscape resistance versus expected resistance effect of environmental predictors under the assumption of disturbance due to artificiality of the predictor or disturbance due to associated human activity and detected resistance pattern

Predictor	Expected effect of the environmental predictor		
	Disturbance due to manmade structures (signs of human neighbourhood)	Disturbance due to human presence (human activity)	Detected resistance/ conductance
Motorways	High resistance	High conductance	High conductance
Railways	Medium resistance	High conductance	High conductance
Green spaces	High conductance	Medium resistance	Low conductance

Laundré, Hernández, & Ripple, 2010). The concept of a "landscape of fear" (Laundré, Hernández, & Altendorf, 2001; Laundré et al., 2010) is frequently applied to foraging behaviour and predator-prey relationships, but the authors promote its consideration for various life history traits. It describes how fear (or predator-induced stress) affects how animals use landscapes. It is not the actual predation risk but the anticipation of risks that limits movement in a landscape of fear (Laundré et al., 2010; Lima, 1998). In the context of our study, this could indicate that human activity drives urban foxes into costly trade-offs as they primarily disperse along structures with little human activity (hence low perceived risk) but high inherent mortality risks. This result conflicts with a model of fearless individuals entering and roaming through the city. Rather, behavioural plasticity may have allowed some foxes to enter the city and facilitate habituation to human presence to some extent, modifying but not obliterating their landscape of fear.

Movement constraints imposed by human activity could be even more relevant for rural foxes that are less accustomed to human presence (see also Stillfried, Gras, et al., 2017). Our results show that rural foxes, unlike their city relatives, do not use artificial structures as dispersal corridors and that dispersal was limited by the city border (Figure 3). It may thus not be the rural foxes' physical capacity to move but the fear to do so that hinders rural foxes from entering the urban island and prevents admixture.

No matter how the genetic differentiation arose, the urban island could persist due to additional behavioural movement limitations. Human presence may thus be the key driver of red fox dispersal behaviour and impact both the separation into rural and urban clusters as well as the dispersal processes within the urban area.

ACKNOWLEDGEMENTS

We are indebted to the Stiftung Naturschutz Berlin as well as the National Natural History Museum of Luxembourg for providing funding. We would like to thank Bill Peterman for his help with the RESISTANCEGA analysis and Gerald Kerth for his support. We further acknowledge the technical staff of LLBB for sampling and four anonymous referees for helping to improve this manuscript.

AUTHOR CONTRIBUTIONS

A.C.F., K.B., and S.E.K. contributed to the design of this research. C.S., K.B., M.H., and U.W. collected the samples. AS and TH performed the laboratory work. C.St., and J.B. contributed to the generation of the resistance surfaces. A.C.F., and S.E.K. conducted data analysis. S.E.K. wrote the manuscript. A.C.F., J.B., M.B., H.H., S.K.S. contributed with substantial revisions to the manuscript.

DATA AVAILABILITY STATEMENT

Microsatellite genotypes, Geographic coordinates, all ascii grid files, and R code for the running of RESISTANCEGA are available on Dryad (https://doi.org/10.5061/dryad.dv41ns1ts).

ORCID

Joscha Beninde https://orcid.org/0000-0002-1677-1809
Anna Schleimer https://orcid.org/0000-0002-9798-5074
Stephanie Kramer-Schadt https://orcid.org/0000-0002-9269-4446
Heribert Hofer https://orcid.org/0000-0002-2813-7442
Christoph Schulze https://orcid.org/0000-0003-1035-3849
Mike Heddergott https://orcid.org/0000-0003-4536-5508
Tanja Halczok https://orcid.org/0000-0002-4471-9290
Alain C. Frantz https://orcid.org/0000-0002-5481-7142

REFERENCES

Adkins, C. A., & Stott, P. (1998). Home ranges, movements and habitat associations of red foxes *Vulpes vulpes* in suburban Toronto, Ontario, Canada. *Journal of Zoology*, *244*(3), 335–346. https://doi.org/10.1111/j.1469-7998.1998.tb00038.x

Balkenhol, N., Waits, L. P., & Dezzani, R. J. (2009). Statistical approaches in landscape genetics: An evaluation of methods for linking landscape and genetic data. *Ecography*, *32*(5), 818–830. https://doi.org/10.1111/j.1600-0587.2009.05807.x

Bateman, P. W., & Fleming, P. A. (2012). Big city life: Carnivores in urban environments. *Journal of Zoology*, *287*, 1–23. https://doi.org/10.1111/j.1469-7998.2011.00887.x

Bates, D., Mächler, M., Bolker, B., & Walker, S. (2014). Fitting linear mixed-effects models using lme4. ArXiv Preprint ArXiv:1406.5823.

Belkhir, K. (2004). 1996–2004 GENETIX 4.05, logiciel sous Windows TM pour la genetique des populations. http://www.genetix.univ-montp2.fr/genetix/intro.htm

Beninde, J., Feldmeier, S., Veith, M., & Hochkirch, A. (2018). Admixture of hybrid swarms of native and introduced lizards in cities is determined by the cityscape structure and invasion history. *Proceedings of the Royal Society B: Biological Sciences*, *285*(1883), 20180143. https://doi.org/10.1098/rspb.2018.0143

Beninde, J., Feldmeier, S., Werner, M., Peroverde, D., Schulte, U., Hochkirch, A., & Veith, M. (2016). Cityscape genetics: Structural vs. functional connectivity of an urban lizard population. *Molecular Ecology*, *25*(20), 4984–5000.

Blanchong, J. A., Sorin, A. B., & Scribner, K. T. (2013). Genetic diversity and population structure in urban white-tailed deer. *The Journal of*

Wildlife Management, *77*(4), 855–862. https://doi.org/10.1002/jwmg.521

Bohonak, A. J. (1999). Dispersal, gene flow, and population structure. *The Quarterly Review of Biology*, *74*(1), 21–45. https://doi.org/10.1086/392950

Börner, K. (2014). Untersuchungen zur Raumnutzung des Rotfuchses, Vulpes vulpes (L., 1758), in verschieden anthropogen beeinflussten Lebensräumen Berlins und Brandenburgs, Doctoral Dissertation. https://doi.org/10.13140/RG.2.1.4336.9200

Börner, K., Wittstatt, U., & Schneider, R. (2009). Untersuchungen zur Populationsökologie des Rotfuchses (Vules vulpes L.) in Berlin. *Beitrg. Jagd- und Wildforsch.*, *34*, 307–313.

Bowcock, A. M., Ruiz-Linares, A., Tomfohrde, J., Minch, E., Kidd, J. R., & Cavalli-Sforza, L. L. (1994). High resolution of human evolutionary trees with polymorphic microsatellites. *Nature*, *368*, 455. https://doi.org/10.1038/368455a0

Breen, M., Jouquand, S., Renier, C., Mellersh, C. S., Hitte, C., Holmes, N. G., … Bristow, A. E. (2001). Chromosome-specific single-locus FISH probes allow anchorage of an 1800-marker integrated radiation-hybrid/linkage map of the domestic dog genome to all chromosomes. *Genome Research*, *11*(10), 1784–1795. https://doi.org/10.1101/gr.189401

Carrete, M., Martínez-Padilla, J., Rodríguez-Martínez, S., Rebolo-Ifrán, N., Palma, A., & Tella, J. L. (2016). Heritability of fear of humans in urban and rural populations of a bird species. *Scientific Reports*, *6*, 31060. https://doi.org/10.1038/srep31060

Carrete, M., & Tella, J. L. (2009). Individual consistency in flight initiation distances in burrowing owls: A new hypothesis on disturbance-induced habitat selection. *Biology Letters*, *6*(2), 167–170. https://doi.org/10.1098/rsbl.2009.0739

Clarke, R. T., Rothery, P., & Raybould, A. F. (2002). Confidence limits for regression relationships between distance matrices: Estimating gene flow with distance. *Journal of Agricultural, Biological, and Environmental Statistics*, *7*(3), 361. https://doi.org/10.1198/1085711102320

Combs, M., Puckett, E. E., Richardson, J., Mims, D., & Munshi-South, J. (2018). Spatial population genomics of the brown rat (*Rattus norvegicus*) in New York City. *Molecular Ecology*, *27*(1), 83–98.

Cushman, S. A., McKelvey, K. S., Hayden, J., & Schwartz, M. K. (2006). Gene flow in complex landscapes: Testing multiple hypotheses with causal modeling. *The American Naturalist*, *168*(4), 486–499. https://doi.org/10.1086/506976

DeCandia, A. L., Brzeski, K. E., Heppenheimer, E., Caro, C. V., Camenisch, G., Wandeler, P., … vonHoldt, B. M. (2019). Urban colonization through multiple genetic lenses: The city-fox phenomenon revisited. *Ecology and Evolution*, *9*(4), 2046–2060. https://doi.org/10.1002/ece3.4898

Dieringer, D., & Schlötterer, C. (2003). Microsatellite analyser (MSA): a platform independent analysis tool for large microsatellite data sets. *Molecular ecology notes*, *3*(1), 167–169.

Dytham, C. (2011). *Choosing and using statistics: A Biologist's guide*, 3rd ed. Hoboken, NJ: Wiley Publishing.

Frantz, A. C., Do Linh San, E., Pope, L. C., & Burke, T. (2010). Using genetic methods to investigate dispersal in two badger (*Meles meles*) populations with different ecological characteristics. *Heredity*, *104*(5), 493–501. https://doi.org/10.1038/hdy.2009.136

Frantz, A. C., Cellina, S., Krier, A., Schley, L., & Burke, T. (2009). Using spatial Bayesian methods to determine the genetic structure of a continuously distributed population: clusters or isolation by distance? *Journal of Applied Ecology*, *46*(2), 493–505.

Frantz, A. C., Pourtois, J. T., Heuertz, M., Schley, L., Flamand, M. C., Krier, A., … Burke, T. (2006). Genetic structure and assignment tests demonstrate illegal translocation of red deer (*Cervus elaphus*) into a continuous population. *Molecular Ecology*, *15*(11), 3191–3203. https://doi.org/10.1111/j.1365-294X.2006.03022.x

Gloor, S. (2002). *The rise of urban foxes* (Vulpes vulpes) *in Switzerland and ecological and parasitological aspects of a fox population in the recently colonised city of Zurich*. Doctoral Dissertation. Zurich, Switzerland: Universitaet Zurich.

Gloor, S., Bontadina, F., Hegglin, D., Deplazes, P., & Breitenmoser, U. (2001). The rise of urban fox populations in Switzerland. *Mamm. biol.*, *66*, 155–164.

Goldingay, R. L., Harrisson, K. A., Taylor, A. C., Ball, T. M., Sharpe, D. J., & Taylor, B. D. (2013). Fine-scale genetic response to landscape change in a gliding mammal. *PLoS ONE*, *8*(12), e80383. https://doi.org/10.1371/journal.pone.0080383

Gortat, T., Rutkowski, R., Gryczynska, A., Kozakiewicz, A., & Kozakiewicz, M. (2017). The spatial genetic structure of the yellow-necked mouse in an urban environment – a recent invader vs. a closely related permanent inhabitant. *Urban Ecosystems*, *20*(3), 581–594. https://doi.org/10.1007/s11252-016-0620-7

Goslee, S. C., & Urban, D. L. (2007). The ecodist package for dissimilarity-based analysis of ecological data. *Journal of Statistical Software*, *22*(7). 1-19, https://doi.org/10.18637/jss.v022.i07

Gruenreich, D. (1992). *ATKIS-a topographic information system as a basis for GIS and digital cartography in Germany*. From Digital Map Series to Geo-Information Systems, Geologisches Jarhrbuch Series A. Hannover, Germany: Federal Institute of Geosciences and Resources.

Guillot, G., Estoup, A., Mortier, F., & Cosson, J.-F. (2005). A spatial statistical model for landscape genetics. *Genetics*, *170*(3), 1261–1280. https://doi.org/10.1534/genetics.104.033803

Guillot, G., Leblois, R., Coulon, A., & Frantz, A. C. (2009). Statistical methods in spatial genetics. *Molecular Ecology*, *18*(23), 4734–4756. https://doi.org/10.1111/j.1365-294X.2009.04410.x

Hardy, O. J., & Vekemans, X. (2002). SPAGeDi: a versatile computer program to analyse spatial genetic structure at the individual or population levels. *Molecular ecology notes*, *2*(4), 618–620.

Harris, S., & Trewhella, W. J. (1988). An Analysis of Some of the Factors Affecting Dispersal in an Urban Fox (*Vulpes vulpes*) Population. *Journal of Applied Ecology*, *25*(25), 409–422. https://doi.org/10.2307/2403833

Janko, C., Linke, S., Romig, T., Thoma, D., Schröder, W., & König, A. (2011). Infection pressure of human alveolar echinococcosis due to village and small town foxes (*Vuples vulpes*) living in close proximity to residents. *European Journal of Wildlife Research*, *57*(5), 1033–1042. https://doi.org/10.1007/s10344-011-0515-0

Johnson, M. T. J., & Munshi-South, J. (2017). Evolution of life in urban environments. *Science*, *358*(6363). https://doi.org/10.1126/science.aam8327

Jombart, T. (2008). Adegenet: A R package for the multivariate analysis of genetic markers. *Bioinformatics (Oxford, England)*, *24*(11), 1403–1405. https://doi.org/10.1093/bioinformatics/btn129

Kauhala, K., Talvitie, K., & Vuorisalo, T. (2016). Encounters between medium-sized carnivores and humans in the city of Turku, SW Finland, with special reference to the red fox. *Mammal Research*, *61*(1), 25–33. https://doi.org/10.1007/s13364-015-0250-0

Khimoun, A., Peterman, W., Eraud, C., Faivre, B., Navarro, N., & Garnier, S. (2017). Landscape genetic analyses reveal fine-scale effects of forest fragmentation in an insular tropical bird. *Molecular Ecology*, *26*(19), 4906–4919. https://doi.org/10.1111/mec.14233

Kivimäki, I., Shimbo, M., & Saerens, M. (2014). Developments in the theory of randomized shortest paths with a comparison of graph node distances. *Physica A: Statistical Mechanics and Its Applications*, *393*, 600–616. https://doi.org/10.1016/j.physa.2013.09.016

Koen, E. L., Garroway, C. J., Wilson, P. J., & Bowman, J. (2010). The effect of map boundary on estimates of landscape resistance to animal movement. *PLoS ONE*, *5*(7), e11785. https://doi.org/10.1371/journal.pone.0011785

Kolb, H. (1984). Factors Affecting the Movements of Dog Foxes in Edinburgh. *Journal of Applied Ecology*, *21*(1), 161–173. https://doi.org/10.2307/2403044

Landguth, E. L., Cushman, S. A., Schwartz, M. K., McKelvey, K. S., Murphy, M., & Luikart, G. (2010). Quantifying the lag time to detect barriers in landscape genetics. *Molecular Ecology*, *19*(19), 4179–4191. https://doi.org/10.1111/j.1365-294X.2010.04808.x

Latch, E. K., Dharmarajan, G., Glaubitz, J. C., & Rhodes, O. E. (2006). Relative performance of Bayesian clustering software for inferring population substructure and individual assignment at low levels of population differentiation. *Conservation Genetics*, *7*(2), 295–302. https://doi.org/10.1007/s10592-005-9098-1

Laundré, J. W., Hernández, L., & Altendorf, K. B. (2001). Wolves, elk, and bison: Reestablishing the" landscape of fear" in Yellowstone National Park, USA. *Canadian Journal of Zoology*, *79*(8), 1401–1409. https://doi.org/10.1139/z01-094

Laundré, J. W., Hernández, L., & Ripple, W. J. (2010). The Landscape of Fear: Ecological Implications of Being Afraid. *The Open Ecology Journal*, *2*, 1–7.

Lima, S. L. (1998). Stress and decision making under the risk of predation: Recent developments from behavioral, reproductive, and ecological perspectives. *Advances in the Study of Behavior*, *27*, 215–290.

Lourenço, A., Álvarez, D., Wang, I. J., & Velo-Antón, G. (2017). Trapped within the city: Integrating demography, time since isolation and population-specific traits to assess the genetic effects of urbanization. *Molecular Ecology*, *26*(6), 1498–1514. https://doi.org/10.1111/mec.14019

Manel, S., & Holderegger, R. (2013). Ten years of landscape genetics. *Trends in Ecology & Evolution*, *28*(10), 614–621. https://doi.org/10.1016/j.tree.2013.05.012

Mariat, D., Amigues, Y., & Boscher, M. Y. (1998). Eight canine tetranucleotide repeats. *Animal Genetics*, *29*(2), 156–157.

McRae, B. H. (2006). Isolation by resistance. *Evolution*, *60*(8), 1551–1561. https://doi.org/10.1111/j.0014-3820.2006.tb00500.x

McRae, B., Shah, V., & Mohapatra, T. (2013). CIRCUITSCAPE *User Guide 4. How Circuitscape Works*. Seattle WA: The Nature Conservancy.

Miller, M. P. (2005). Alleles In Space (AIS): Computer software for the joint analysis of interindividual spatial and genetic information. *Journal of Heredity*, *96*(6), 722–724. https://doi.org/10.1093/jhered/esi119

Møller, A. P. (2009). Successful city dwellers: A comparative study of the ecological characteristics of urban birds in the Western Palearctic. *Oecologia*, *159*(4), 849–858. https://doi.org/10.1007/s00442-008-1259-8

Møller, A. P., Tryjanowski, P., Díaz, M., Kwieciński, Z., Indykiewicz, P., Mitrus, C., … Polakowski, M. (2015). Urban habitats and feeders both contribute to flight initiation distance reduction in birds. *Behavioral Ecology*, *26*(3), 861–865. https://doi.org/10.1093/beheco/arv024

Montero, E., Van Wolvelaer, J., & Garzón, A. (2014). The European urban atlas. In: I. Manakos & M. Braun (Eds.). *Land use and land cover mapping in Europe* (pp. 115–124). Dordrecht, The Netherlands: Springer.

Moore, M., Brown, S. K., & Sacks, B. N. (2010). Thirty-one short red fox (*Vulpes vulpes*) microsatellite markers. *Molecular Ecology Resources*, *10*, 404–408.

Munshi-South, J. (2012). Urban landscape genetics: Canopy cover predicts gene flow between white-footed mouse (*Peromyscus leucopus*) populations in New York City. *Molecular Ecology*, *21*(6), 1360–1378.

Nei, M., & Takezaki, N. (1983). Estimation of genetic distances and phylogenetic trees from DNA analysis. In C. Smith (Ed.), *Proceedings of the 5th World Cong Genet Appl Livestock Production*, Vol. *21* (pp. 405–412). Guelph, ON: University of Guelph, Canada.

Peterman, W. E. (2018). RESISTANCEGA: An R package for the optimization of resistance surfaces using genetic algorithms. *Methods in Ecology and Evolution*, *9*(6), 1638–1647.

Petkova, D., Novembre, J., & Stephens, M. (2016). Visualizing spatial population structure with estimated effective migration surfaces. *Nature Genetics*, *48*(1), 94. https://doi.org/10.1038/ng.3464

Pritchard, J. K., Stephens, M., & Donnelly, P. (2000). Inference of population structure using multilocus genotype data. *Genetics*, *155*(2), 945–959. https://doi.org/10.1111/j.1471-8286.2007.01758.x

Prunier, J. G., Colyn, M., Legendre, X., Nimon, K. F., & Flamand, M. C. (2015). Multicollinearity in spatial genetics: Separating the wheat from the chaff using commonality analyses. *Molecular Ecology*, *24*(2), 263–283. https://doi.org/10.1111/mec.13029

Puechmaille, S. J. (2016). The program structure does not reliably recover the correct population structure when sampling is uneven: Subsampling and new estimators alleviate the problem. *Molecular Ecology Resources*, *16*(3), 608–627.

Richardson, J. L., Brady, S. P., Wang, I. J., & Spear, S. F. (2016). Navigating the pitfalls and promise of landscape genetics. *Molecular Ecology*, *25*(4), 849–863. https://doi.org/10.1111/mec.13527

Riley, S. P. D., Pollinger, J. P., Sauvajot, R. M., York, E. C., Bromley, C., Fuller, T. K., & Wayne, R. K. (2006). A southern California freeway is a physical and social barrier to gene flow in carnivores. *Molecular Ecology*, *15*(7), 1733–1741. https://doi.org/10.1111/j.1365-294X.2006.02907.x

Rodríguez-Ramilo, S. T., & Wang, J. (2012). The effect of close relatives on unsupervised Bayesian clustering algorithms in population genetic structure analysis. *Molecular Ecology Resources*, *12*(5), 873–884. https://doi.org/10.1111/j.1755-0998.2012.03156.x

Rousset, F. (2008). GENEPOP'007: A complete re-implementation of the GENEPOP software for Windows and Linux. *Molecular Ecology Resources*, *8*(1), 103–106. https://doi.org/10.1111/j.1471-8286.2007.01931.x

Rowe, G., & Beebee, T. J. C. (2007). Defining population boundaries: Use of three Bayesian approaches with microsatellite data from British natterjack toads (*Bufo calamita*). *Molecular Ecology*, *16*(4), 785–796. https://doi.org/10.1111/j.1365-294X.2006.03188.x

Ruiz-Lopez, M. J., Barelli, C., Rovero, F., Hodges, K., Roos, C., Peterman, W. E., & Ting, N. (2016). A novel landscape genetic approach demonstrates the effects of human disturbance on the Udzungwa red colobus monkey (*Procolobus gordonorum*). *Heredity*, *116*(2), 167–176. https://doi.org/10.1038/hdy.2015.82

Saar, C. (1957). *Parasitologische Untersuchungen beim Rotfuchs (*Vulpes vulpes*) im Raum von West-Berlin*. Berlin, Germany: Institut Parasitologie, Freie Universitaet Berlin.

Samia, D. S. M., Nakagawa, S., Nomura, F., Rangel, T. F., & Blumstein, D. T. (2015). Increased tolerance to humans among disturbed wildlife. *Nature Communications*, *6*, 8877. https://doi.org/10.1038/ncomms9877

Santonastaso, T. T., Dubach, J., Hauver, S. A., Graser, W. H. III, & Gehrt, S. D. (2012). Microsatellite analysis of raccoon (*Procyon lotor*) population structure across an extensive metropolitan landscape. *Journal of Mammalogy*, *93*(2), 447–455.

Sawyer, S. C., Epps, C. W., & Brashares, J. S. (2011). Placing linkages among fragmented habitats: Do least cost models reflect how animals use landscapes? *Journal of Applied Ecology*, *48*(3), 668–678. https://doi.org/10.1111/j.1365-2664.2011.01970.x

Schwartz, M. K., Copeland, J. P., Anderson, N. J., Squires, J. R., Inman, R. M., McKelvey, K. S., … Cushman, S. A. (2009). Wolverine gene flow across a narrow climatic niche. *Ecology*, *90*(11), 3222–3232. https://doi.org/10.1890/08-1287.1

Scrucca, L. (2013). GA: a package for genetic algorithms in R. *Journal of Statistical Software*, *53*(4), 1–37.

She, J. X., Autemm, M., Kotulas, G., Pasteur, N., & Bonhomme, F. (1987). Multivariate analysis of genetic exchanges between *Solea segalensis* (*Teleosts*, *Soleidae*). *Biological Journal of the Linnean Society*, *32*, 357–371.

Shirk, A. J., Landguth, E. L., & Cushman, S. A. (2017). A comparison of individual-based genetic distance metrics for landscape genetics. *Molecular Ecology Resources*, *17*(6), 1308–1317. https://doi.org/10.1111/1755-0998.12684

Shirk, A. J., Landguth, E. L., & Cushman, S. A. (2018). A comparison of regression methods for model selection in individual-based landscape genetic analysis. *Molecular ecology resources*, *18*(1), 55–67.

Shochat, E., Warren, P. S., Faeth, S. H., McIntyre, N. E., & Hope, D. (2006). From patterns to emerging processes in mechanistic urban ecology. *Trends in Ecology & Evolution*, *21*(4), 186–191. https://doi.org/10.1016/j.tree.2005.11.019

Stillfried, M., Fickel, J., Börner, K., Wittstatt, U., Heddergott, M., Ortmann, S., … Frantz, A. C. (2017). Do cities represent sources, sinks or isolated islands for urban wild boar population structure? *Journal of Applied Ecology*, *54*(1), 272–281. https://doi.org/10.1111/1365-2664.12756

Stillfried, M., Gras, P., Börner, K., Göritz, F., Painer, J., Röllig, K., … Kramer-Schadt, S. (2017). Secrets of success in a landscape of fear: Urban wild boar adjust risk perception and tolerate disturbance. *Frontiers in Ecology and Evolution*, *5*, 15. https://doi.org/10.3389/fevo.2017.00157

Tischendorf, L., & Fahrig, L. (2000). On the usage and measurement of landscape connectivity. *Oikos*, *90*(1), 7–19. https://doi.org/10.1034/j.1600-0706.2000.900102.x

Trewhella, W. J., & Harris, S. (1990). The effect of railway lines on urban fox (*Vulpes vulpes*) numbers and dispersal movements. *Journal of Zoology*, *221*(2), 321–326. https://doi.org/10.1111/j.1469-7998.1990.tb04004.x

Trumbo, D. R., Spear, S. F., Baumsteiger, J., & Storfer, A. (2013). Rangewide landscape genetics of an endemic Pacific northwestern salamander. *Molecular Ecology*, *22*(5), 1250–1266. https://doi.org/10.1111/mec.12168

Tucker, M. A., Böhning-Gaese, K., Fagan, W. F., Fryxell, J. M., Van Moorter, B., Alberts, S. C., … Avgar, T. (2018). Moving in the Anthropocene: Global reductions in terrestrial mammalian movements. *Science*, *359*(6374), 466–469.

Verhoeven, K. J. F., Simonsen, K. L., & McIntyre, L. M. (2005). Implementing false discovery rate control: Increasing your power. *Oikos*, *108*(3), 643–647. https://doi.org/10.1111/j.0030-1299.2005.13727.x

Voigt, D. R., & Macdonald, D. W. (1984). Variation in the spatial and social behaviour of the red fox, *Vulpus vulpes*. *Acta Zoologica Fennica*, *171*, 261–265.

Vuorisalo, T., Talvitie, K., Kauhala, K., Bläuer, A., & Lahtinen, R. (2014). Urban red foxes (*Vulpes vulpes* L.) in Finland: A historical perspective. *Landscape and Urban Planning*, *124*, 109–117. https://doi.org/10.1016/j.landurbplan.2013.12.002

Wandeler, P., & Funk, S. M. (2006). Short microsatellite DNA markers for the red fox (*Vulpes vulpes*). *Molecular Ecology Notes*, *6*(1), 98–100. https://doi.org/10.1111/j.1471-8286.2005.01152.x

Wandeler, P., Funk, S. M., Largiadèr, C. R., Gloor, S., & Breitenmoser, U. (2003). The city-fox phenomenon: Genetic consequences of a recent colonization of urban habitat. *Molecular Ecology*, *12*, 647–656. https://doi.org/10.1046/j.1365-294X.2003.01768.x

Weir, B. S., & Cockerham, C. C. (1984). Estimating F-statistics for the analysis of population structure. *Evolution*, *38*, 1358–1370.

Wilson, A., Fenton, B., Malloch, G., Boag, B., Hubbard, S., & Begg, G. (2016). Urbanisation versus agriculture: A comparison of local genetic diversity and gene flow between wood mouse *Apodemus sylvaticus* populations in human-modified landscapes. *Ecography*, *39*(1), 87–97.

Yan, S. Q., Bai, C. Y., Qi, S. M., Li, Y. M., Li, W. J., & Sun, J. H. (2015). Development of novel polymorphic microsatellite markers for the silver fox (*Vulpes vulpes*). *Genetics and Molecular Research*, *14*(2), 5890–5895. https://doi.org/10.4238/2015.June.1.6

SUPPORTING INFORMATION

Additional supporting information may be found online in the Supporting Information section.

How to cite this article: Kimmig SE, Beninde J, Brandt M, et al. Beyond the landscape: Resistance modelling infers physical and behavioural gene flow barriers to a mobile carnivore across a metropolitan area. *Mol Ecol*. 2020;29:466–484. https://doi.org/10.1111/mec.15345